Memoirs of the Faculty of Engineering, Nagoya University
Vol.42, No.1 (1990)

STUDY ON THE SPATIAL AND TEMPORAL BEHAVIORS OF UNCONFINED GROUNDWATER HEAD-FIELD IN HETEROGENEOUS REGION

Fusetsu TAKAGI and Morihiro HARADA

Department of Civil Engineering

(Received May 31, 1990)

Abstract

The spatial distribution of hydraulic head, namely "head-field", is estimated from a limited set of observed data, including the uncertainty which caused by both the complexity of groundwater behavior due to the heterogeneity of flow region and the insufficiency of measurement equipments. It is necessary for the precise analysis of the regional groundwater to evaluate quantitatively the uncertainty of head-field. The present study is directed toward tackling this problem from stochastic standpoint. The behavior of unconfined head-field in the heterogeneous flow region due to a rainfall is treated as the physical process in the random field, and the statistical structure of head-field is analyzed based on the physical principles of the subsurface flow. Firstly, the spatial randomness of water-table response to a rainfall is formulated as the head variance, taking the infiltration process in unsaturated zone into consideration. Secondly, the unsteady head variogram after the rainfall is theoretically derived by the perturbation expansion, and the spatial head distributions during the recession process are estimated from a limited set of point data through the geostatistical approach. And lastly, a new criterion for the parameter identification of the regional groundwater model is also proposed, which takes full advantage of the stochastic properties on the uncertainty of actual head behavior.

Contents

1. Introduction

In order to analyze the regional groundwater behavior, the primary issues are the problems how to estimate and how to understand actual spatial and temporal distributions of hydraulic head of groundwater. For the actual distributions are the fundamental information for various processes of the analysis, such as the aquifer modelling, the parameter identification, the verification of numerical results. In the investigation of the spatial distribution of head, namely "Head-Field", however, it is rare to obtain available head data enough for a practical analysis, because observation wells are limited in number and in space. Also, temporal behaviors of head-field are generally complex, since the aquifer system is usually heterogeneous

and affected diversely by artificial activities. Consequently, it often happens that head data at some observed wells indicate rather mainly the local singular fluctuations, compared with the spatial scale concerned. In particular, the influence of heterogeneity is important in the unconfined case, and head data at some points just after a heavy rainfall are apt to fluctuate independently to each other.

The purpose of the present study is to clarify physical structure of the randomness of head-field in a heterogeneous region, and to evaluate the uncertainty of head data at observation wells. In this paper, the behavior of unconfined head-field due to a rainfall event is treated as the physical process in non-stationary random field by combining statistical concepts and physical principles.

The present paper consists of the following chapters;

Chapter 2: Through hydrological observations and geological investigations at two experimental basins, the real condition of the heterogeneity in the actual region and the characteristics of fluctuation of the unconfined hydraulic head are discussed. The statistical properties of hydraulic coefficients in the actual aquifer are estimated positively based on field data. The phenomenological discussions on the factors governing the spatial difference of head data are also presented.

Chapter 3: The stochastic evaluation of the uncertainty in "random response process" of head-field to a heavy rainfall is presented. Theoretical formulation of the head variance which expresses statistically the randomness of head-field is made based on physical laws with respect to the vertical unsaturated flow and the horizontal groundwater flow. It has been clarified then how the head variance depends on both flow properties in the unsaturated zone and in the aquifer (saturated zone), and the fact that head-field has greater variance of its spatial distribution in the silty aquifer than in the sandy aquifer is demonstrated.

Chapter 4: The stochastic evaluation of the uncertainty in "smoothing process" of head-field during a long-term recession period after a rainfall is presented. By evaluating the random components of head due to the heterogeneity of aquifer, a theoretical functional form of head variogram, which expresses a spatial structure of head-field is analytically derived from the fundamental flow equations. The unsteady head-field after a rainfall is then stochastically estimated from a limited set of point data with help of the universal kriging method and theoretical variogram. Through the result of the kriging analysis, it is shown that the estimation accuracy of head-field is improved gradually with the passage of time after a rainfall. These facts suggest that the significance of the observed head values in the groundwater analyses will change with the temporal and spatial scales of groundwater behaviors.

Chapter 5: The problem how to apply the hydraulic information obtained by the observation of head to the practical analysis in heterogeneous region is discussed. In previous researches, the aquifer parameters of simulation models have been identified by a direct comparison of the simulated head values with the observed head data. However, it should be noted that the simulated values are macroscopic solutions, while the observed data include local random components caused by the heterogeneity of aquifer. To avoid this difficulty, a new criterion for the parameter identification in the unconfined heterogeneous aquifer is proposed. The criterion proposed takes full advantage of the statistical property on uncertainty of actual head behaviors.

Chapter 6: The conclusions in the present paper are summarized.

2. Field Observation of Hydraulic Head and Heterogeneity of Flow Region

2. 1 Outlines of Experimental Basins and Hydrological Measurement System

Firstly, let us discuss about the field data related to the groundwater head and the hydraulic properties in actual aquifer, to state an outline of the objective phenomena concerned. Two experimental basins A and B for the field investigations have been established in a flat plain area and in a hill slope area, as shown in Fig. 2. 1.

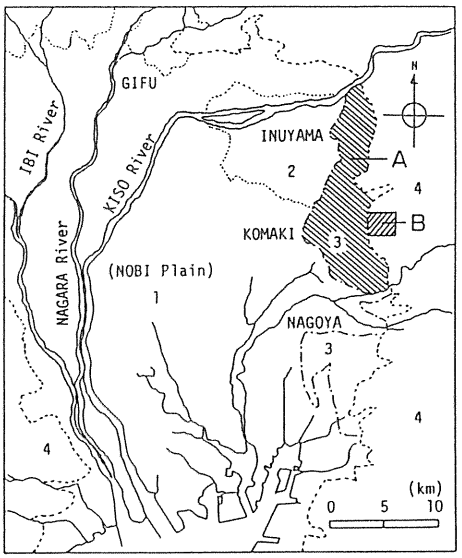

Fig. 2. 1 Location of Basins A and B.

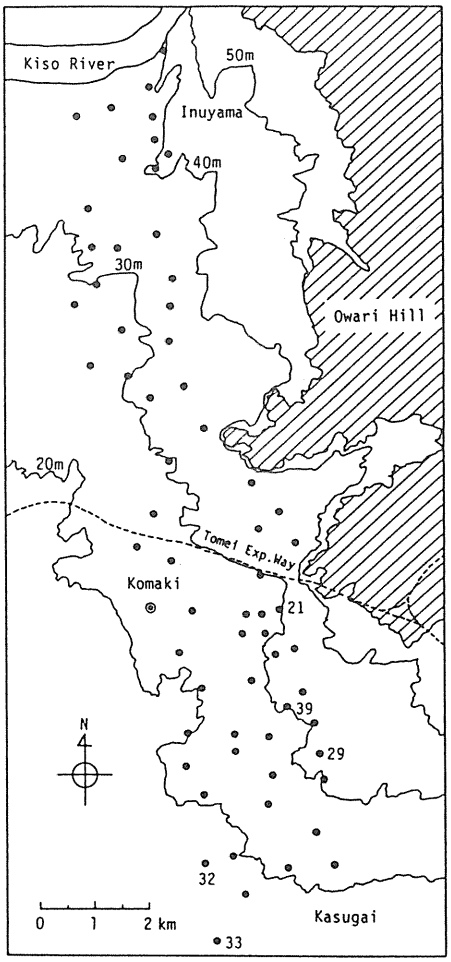

Fig. 2. 2 Experimental Basin A
(●: well, ⊙: raingauge).

Basin A is located at Northern East area of the Nobi Plain, Central Japan, with an area of about 30 km^2. The geomorphology of the basin is the diluvial terras in the most part. Therefore the geology mainly consists of the diluvial formations composed of sandy gravel beds, and it may be understood that this region is geologically uniform. Hydrological installations such as the raingauges and the observation wells are sited in Fig. 2. 2. These wells have

provided the piezometers on the same standard that the inside diameter is 10 cm and the screen depth is G.L. − 20 m. Number of the wells is 67 in all, and the head behavior has been measured continuously by self-recording instruments. The land use in the basin A is mainly a rice field except a few small areas of town.

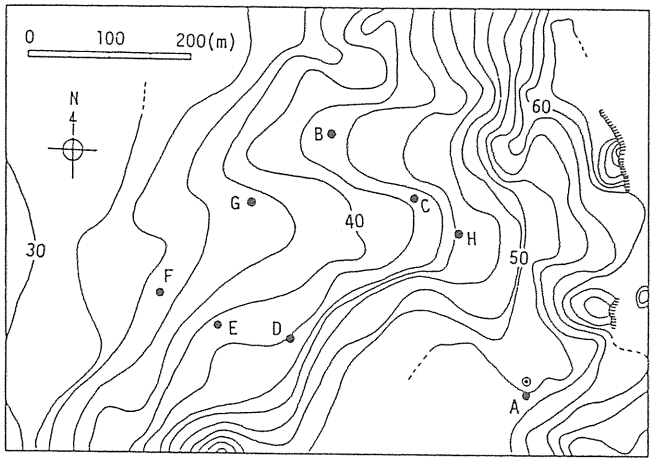

Fig. 2. 3 Experimental Basin B (●: well, ⊙: raingauge).

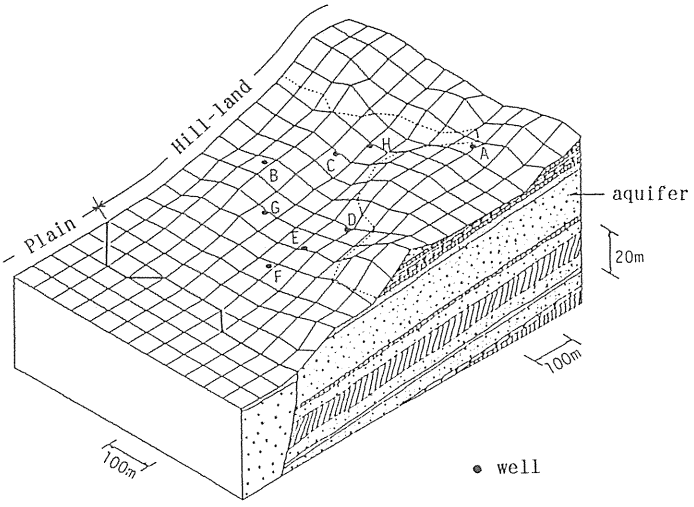

Fig. 2. 4 Geomorphology and Geology of Basin B.

Basin B is established at the Komaki Hill located adjacent to Basin A, with an area of only 0.23 km^2. The geology is Hill-land constituting Tertiary, called the Yadagawa Formation of the Seto group, and consists of sandy gravel beds and silt beds sloping gently down toward the southwest at an angle of about 3°. As shown in Fig. 2. 3, 8 shallow wells and a raingauge

are equipped for the hydrological measurement. The depth of wells are 6 m to 12 m under ground level, and the head behavior observed at these wells is that of groundwater flow in the formation shown in Fig. 2. 4. The land use within Basin B is mixed with the farms and the housing sites. And no withdrawal from the aquifer has been carried out (Takagi et al., 1985).

2. 2 Heterogeneity of Hydraulic Properties in Flow Region

2. 2. 1 Statistical Distribution of Permeability

Within Basin A, the borehole test was carried out at providing the wells to measure the permeability K of aquifer. Usually, in the borehole test, the rising heights or the fluctuations of head in the hole are measured when a quantity of water is injected into the hole, and many sort of formula are used to calculate the permeability. Fig. 2. 5 shows the results of the test plotted on a probability paper. From this figure, it appears that point values of permeability scatter within a range of some orders and follow the lognormal distribution as a whole, even though the region is geologically uniform in macroscopic meaning. This statistical property of permeability has been also pointed out by several researchers. The standard deviations of the lognormal distribution have been reported as 0.2 to 1.6 in 20 basins by Freeze (1975) and 0.13 to 1.0 in 13 basins by Delhomme (1979). In this Basin A the standard deviation of log K is 0.89. The differences among these values seem to depend on the difference of geology and by the measurement methods of permeability. However, it can infer the fact that log K data on local scale distribute normally in any groundwater basins.

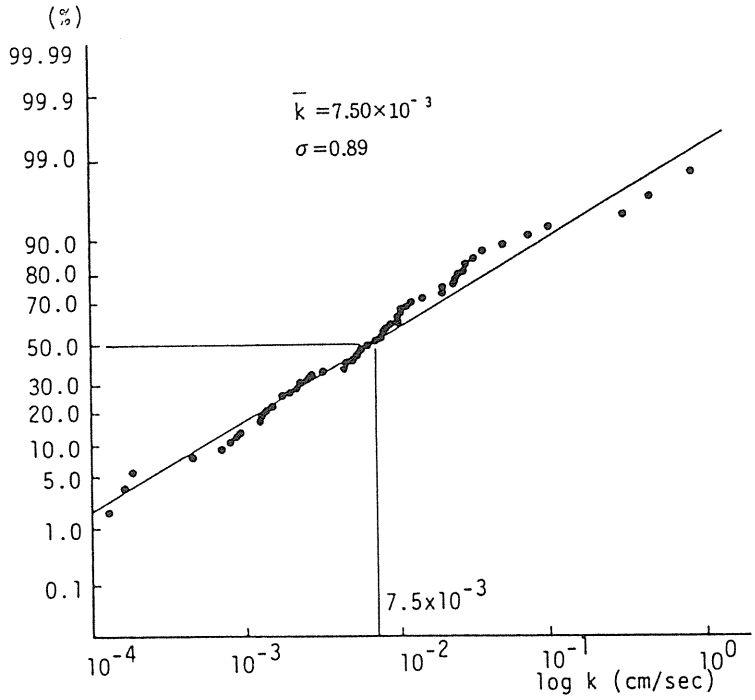

Fig. 2. 5 Lognormal distribution of permeability by the borehole tests.

2. 2. 2 Spatial Structure of Permeability Data in Basin A

In order to investigate the spatial characteristic of the heterogeneity in the flow region, a variogram of permeability data obtained by the borehole test was estimated. The variogram is a statistical function defined as Eq. (1) and represents both the randomness and the spatial correlation.

$$\gamma(d_{ij}) = \frac{1}{2} Var[Z(X_i) - Z(X_j)] , \quad d_{ij} = | X_i - X_j | \tag{1}$$

where X denotes a location vector, $Z(X)$ is random variable at a point X and d_{ji} is distance between any points X_i and X_j. Here, the logarithm of permeability $K(X)$ is adopted as the random variable $Z(X)$. In actual calculation, the distances between two observation points are classified every 1.5 km, and the number of pairs with the same distance d_{ij}, $N(d_{ij})$, is shown in Table 2. 1. Since values of $N(d)$ is closely related to the reliability of the variogram, the variogram is drawn for the range of $d_{ij} > 13.5$ km that corresponds to the range of $N(d) > 50$. Fig. 2. 6 shows the variogram of log K based on the following equation, under the stationary hypothesis.

Table 2. 1 Values of the number of point-pairs $N(d)$.

d	0.0-1.5	1.5-3.0	3.0-4.5	4.5-6.0	6.0-7.5	7.5-9.0	9.0-10.5	10.5-12	12-13.5	13.5-15	15-16.5
N	154	291	199	147	142	129	119	99	64	27	7

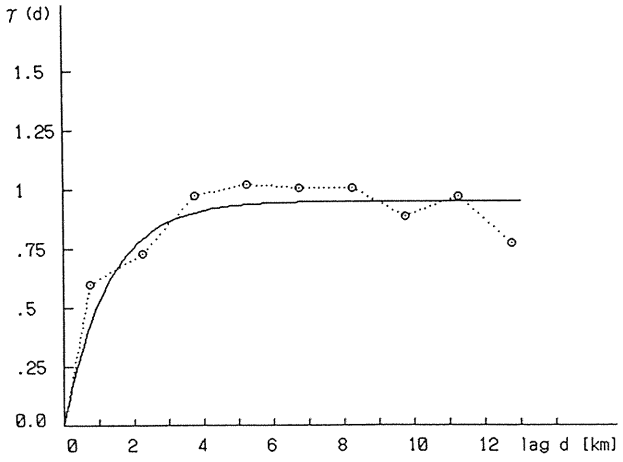

Fig. 2. 6 Statistical spatial structure of permeability (Basin A).

$$\gamma(d_{ij}) = \frac{1}{2\,N(d_{ij})} \sum_{ij} [Z(X_i) - Z(X_j)]^2 \qquad (2)$$

In this figure, the spatial correlation of permeability from the borehole test is relatively small. Therefore, the spatial distribution of the hydraulic properties at each point in the regional scale is inferred to be independent on one another.

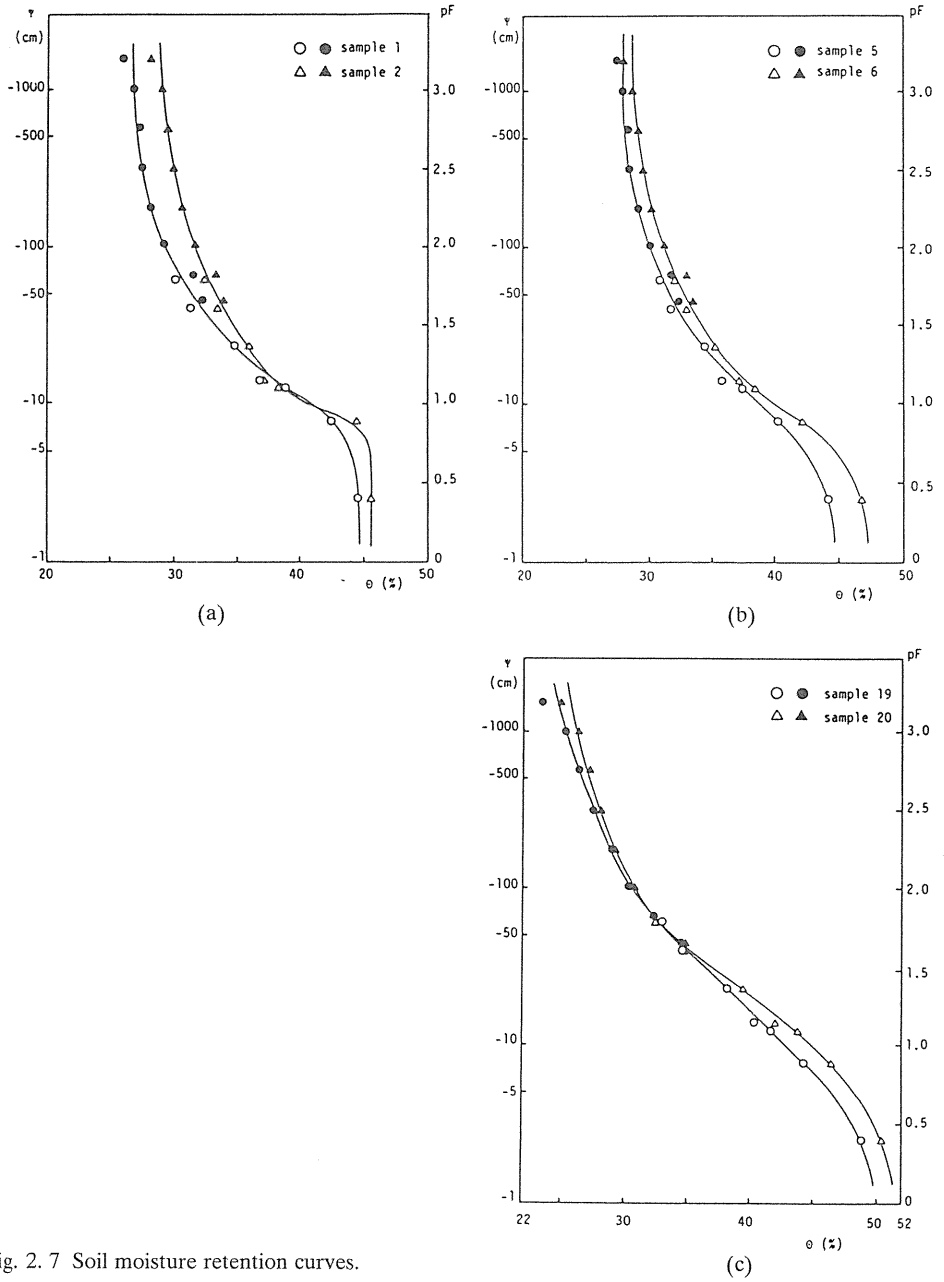

Fig. 2. 7 Soil moisture retention curves.

2. 2. 3 *Unsaturated Moisture Property of Soil and Specific Yield*

Since the unsaturated flow in soil zone is closely related to the recharge to groundwater table and the fluctuation of water-table, it is necessary for discussion of the head behavior due to the infiltration of rain-water to clarify the physical properties of unsaturated soil. In Basin B, a large number of soil samples were extracted from the shallow layer of the natural ground, and their unsaturated property and the specific yield were investigated through the laboratory tests.

In the test for the unsaturated property of soil, the moisture retention curve is usually identified, which indicates the relationship between the volumetric moisture content θ and the capillary head ψ. In this test, two methods are used according to the range of tension. That is, the soil column method for low tension range (pF(=log ψ) 0 to 1.8) and the pressure plate method for high tension range (pF 1.5 to 3.2). Examples of test results are shown in Fig. 2. 7. In the figures, symbols ○ and △ indicate the data by the soil column method, and symbols ● and ▲ are data by the pressure plate method, respectively. As may be seen from these results, the moisture retention characteristics indicated by the pF-θ curve are different among the sampling points. The effective porosity of each sample estimated by pF-θ curves averages the value of 10 percent in its distribution and fluctuates in the range 5 to 20 percent. In other words, this fact means that the soil zone is greatly heterogeneous in its storativity in the actual region.

2. 3 *Phenomenological Discussion on Head Behavior due to Rainfall*

According to the field observation, the head responce process to rainfall is a phenomenon of a few-days-scale, while the head recession after rainfall is gradually changing process in rather long-term. In this section, then, we discuss these two processes separately.

In the region concerned, we had a heavy storm of daily rainfall exceeded 100 mm in September 1983. The behavior of groundwater-table in this rainfall occasion has been observed as shown in Fig. 2. 8 for 5 shallow wells in Basin A. This figure shows that the water-table in each well rises simultaneously and reaches at its peak level at almost the same time all over the region. However, the rising height of head differs considerably from point to point in the region, strongly affected by the heterogeneity of flow domain. The maximum rising height of head ΔH is shown in Fig. 2. 9 versus the depth of water-table Dp under the ground surface just before the rainfall. The scattering of the plots in the figure implies that the differences of head rising are independent on the length of unsaturated zone. Thus, we face to the new problem what quantity may result in this difference in the head rising.

The same phenomena as in Basin A, are also observed in Basin B. Fig. 2. 10 shows the rising heights in 5 wells to another momentary heavy storm. As known from the figure, the head in each well responses variously from a steep rising to a mild one even in so small region.

While in the long dry period, in the Basins A and B, where the aquifer is mainly recharged by the rain-water, the unconfined water-table falls gradually down. For examples, the head fluctuations during about 4 dry months after the storm in September 1983 are shown in Fig. 2. 11 (Basin A) and Fig. 2. 12 (Basin B). Although the head behaviors just after the rainfall are very different one another, the falling rates of heads after the rainfall become similar to each other with passage of time. This fact indicates that the local components of head fluctuation are reduced for the dry period, and that the macroscopic behavior in the whole region appears at each well.

The groundwater behavior described above may be summarized conceptually as a phenomenon shown in Fig. 2. 13. The head-field in a heterogeneous region becomes random by a heavy rainfall (in Fig. 2. 13(a) to Fig. (b)). After that, the head-field smooths down during

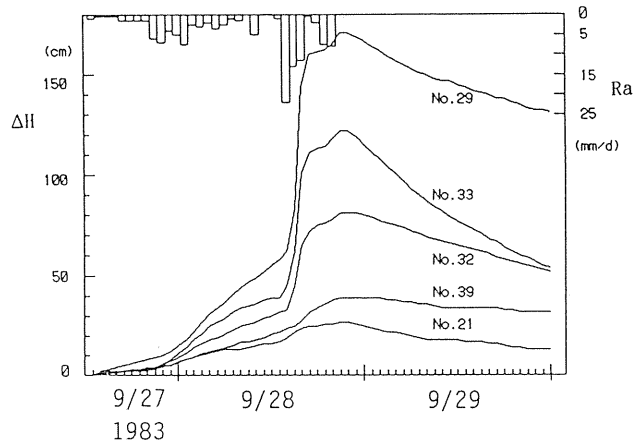

Fig. 2. 8 Rising process of head due to rainfall (Basin A).

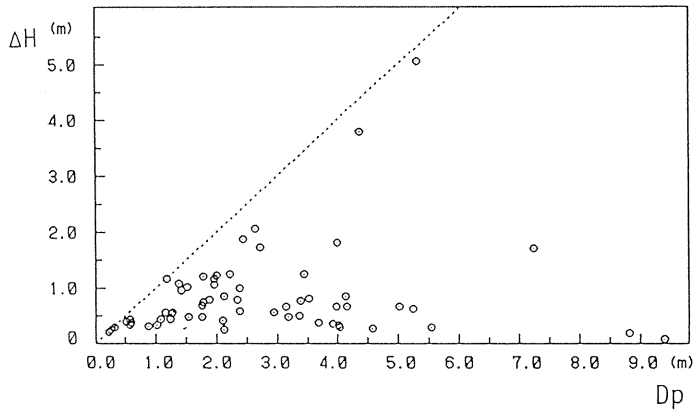

Fig. 2. 9 Relationship between ΔH and Dp (Basin A).

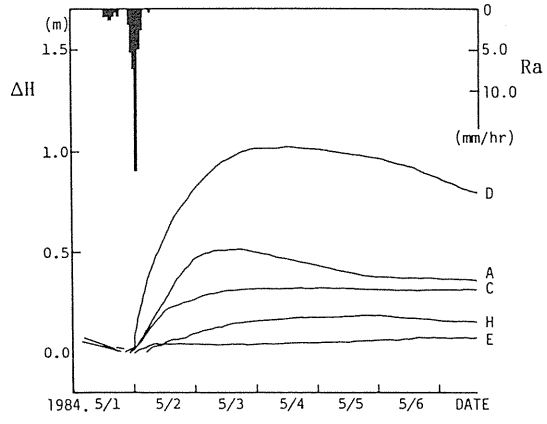

Fig. 2. 10 Rising process of head due to rainfall (Basin B).

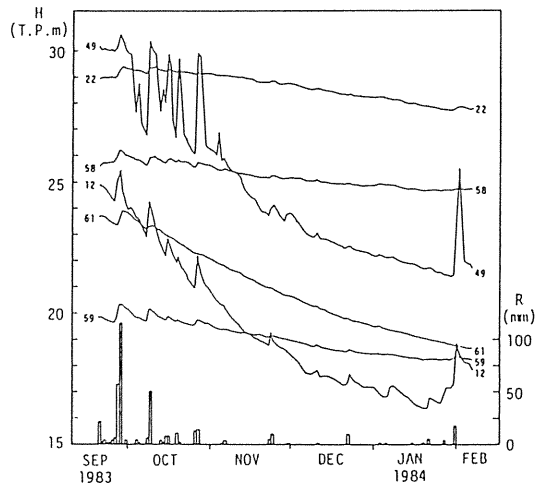

Fig. 2. 11 Recession process of head during a long dry period (Basin A).

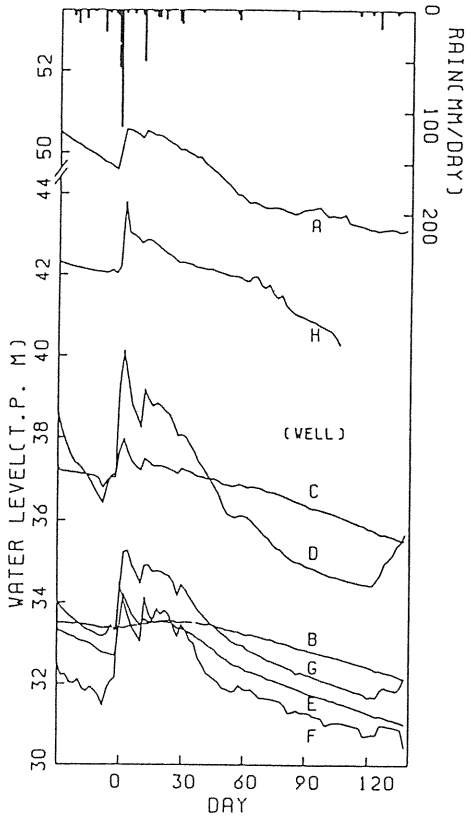

Fig. 2. 12 Recession process of head during a long dry period (Basin B).

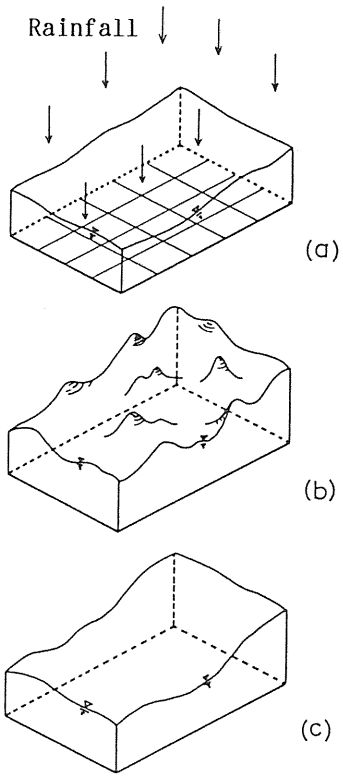

Fig. 2. 13 Random behavior of head-field caused by a rainfall.

a dry period and recovers the calmness before the rainfall (in Fig. (b) to Fig. (c)). After all, the head observation at wells is no more than a look at this complex behavior of head-field through peepholes. By regarding this head behavior as the physical phenomena in a random field, the stochastic characteristics of unsteady head-field are analyzed in the following chapter, based on physical principles in both the response process to a rainfall and the recession process after the rainfall.

3. Stochastic Analysis of Response Process of Head-Field to Rainfall

3. 1 Uncertain Factors in Head Rising Phenomena

The head response to rainfall is the phenomenon that the water-table rises due to the increasing storage of groundwater flow by the recharge of rain-water, as shown in Fig. 3. 1. In the case that the thickness of unsaturated zone to water-table D is large in comparison with the rising height of water-table Δh, the head response process to rainfall may be separated

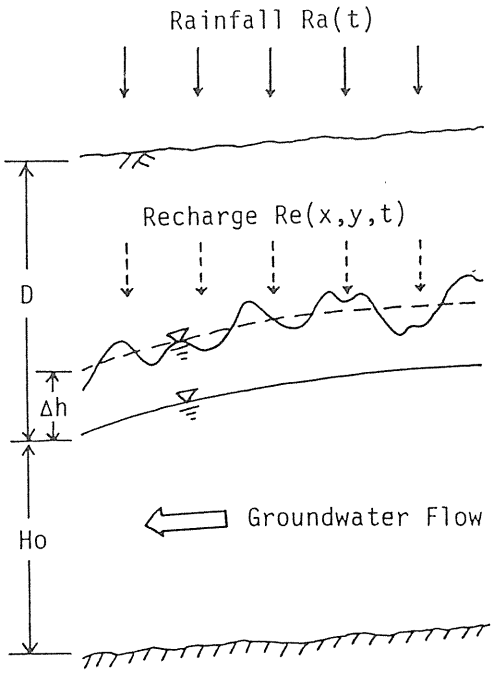

Fig. 3. 1 Schematic illustration of head rising phenomena.

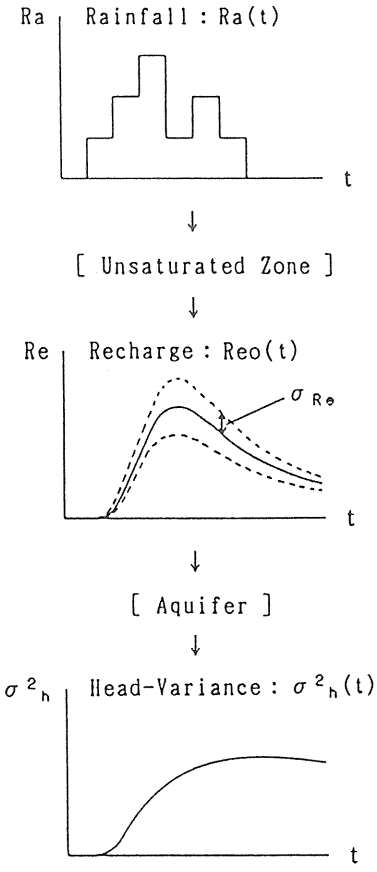

Fig. 3. 2 Relations among rainfall, recharge and head variance.

into the following two processes: the vertical seepage process in unsaturated zone and the head rising process in aquifer. Fig. 3. 2 illustlates schematically these processes from rainfall to response of head. In this figure, the rainwater infiltrates vertically from the ground surface with intensity $Ra(t)$. The seepage water is affected by some transformation in unsaturated zone and reaches at the groundwater-table as the recharge to aquifer with intensity $Re(t)$. If the soil zone is isotropic and homogeneous, $Re(t)$ is spatially constant in whole region. However, in heterogeneous case, Re becomes random variable $Re(x,y,t)$ with average value $Re_0(t)$ and spatial variance $\sigma^2_{Re}(t)$. In this paper, such the heterogeneous region that its hydraulic properties are assumed to fluctuate a little around the average values is considered. Although the groundwater head at each point intends to rise independently corresponding to $Re(x,y,t)$ at its point, the randomness of head-field is relaxed due to the diffusion effect caused by the lateral flow process in aquifer. These processes in both the unsaturated zone and the aquifer result in the head response with the spatial variance $\sigma^2_h(t)$.

3. 2 Groundwater Recharge Process through Heterogeneous Soil Zone

Transformation process from the rainfall intensity $Ra(t)$ to the recharge intensity $Re(x,y,t)$ is analyzed by the unsaturated flow theory based on the Richards' equation. The Richards' equation is a modelling of the moisture movement in the unsaturated soil, based on a concept of the capillary potential (Richards, 1931). For the analysis of soil moisture, it is necessary to combine this equation with the physical properties of soil, for example, the relationships among the volumetric moisture content θ, the capillary head ψ and the unsaturated permeability K. In actual analysis, ploblems are usually solved through numerical procedures because of the strong non-linearity of the Richards' equation. Certainly, the numerical procedures are an useful arms which can express the complex behavior rather exactly, if the calculation conditions and the soil properties are clearly given. However, the problem to be considered in this chapter is to evaluate the spatial fluctuation of the recharge intensity to aquifer, which causes the random behavior of head. Therefore, the attention should be focused to extract the governing factors of the phenomena and to represent their interrelationships in some analytical form. In this section, at first, the recharge intensity $Re_0(t)$ through homogeneous soil is evaluated by an analytical approximate model of the infiltration, proposed by Dagan & Bresler (1983). And then, the physical structure of the spatial fluctuation of $Re(x,y,t)$ through heterogeneous soil is discussed based on the representation of $Re_0(t)$.

3. 2. 1 Approximate Model of Recharge through Homogeneous Soil

The equation of continuity on the moisture movement in unsaturated soil takes the following form for the one-dimensional vertical flow.

$$\frac{\partial\theta(z,t)}{\partial t} = -\frac{\partial q(z,t)}{\partial z} \tag{3}$$

where q is the vertical flux of soil moisture, z is the vertical downward axis from ground surface, and t is the time. As shown in Fig. 3. 3(a), let us consider the soil moisture profile in the infiltration process of rain-water into the unsaturated soil where the gravitational drainage has almost finished.

Integrating Eq. (3) with respect to z from the ground surface to the wetting front by considering the time advance of the wetting front,

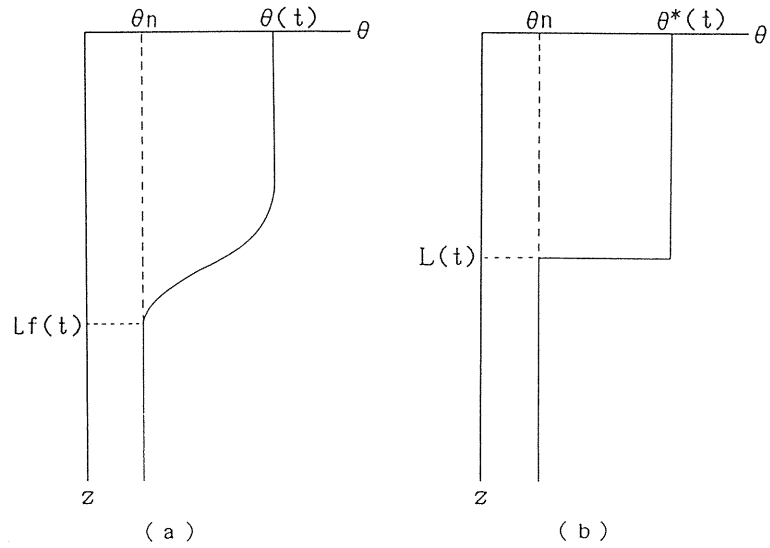

Fig. 3. 3 Approximation of moisture profile in unsaturated soil.

$$\frac{\partial}{\partial t} = \int_0^{L_f(t)} [\theta(z,t) - \theta_n]\, dz = - q(L_f,t) + q(0,t) \tag{4}$$

where θ_n is the field capacity (approximate constant), and $L_f(t)$ is the depth to the wetting front which satisfies the condition: $\theta(L_f,t)=\theta_n$.

For the sake of simplification, the actual θ profile in Fig. 3. 3(a) is replaced by the equivalent one of constant θ^* as shown in Fig. 3. 3(b). θ^* and $L(t)$ are defined here for equivalent condition of increasing value of the moisture from the ground surface to the wetting front, that is

$$V(t) = \int_0^{L_f(t)} [\theta(z,t) - \theta_n]\, dz = [\theta^*(t) - \theta_n] L(t) \tag{5}$$

From Eqs. (4) and (5), we obtain

$$q(0,t) - q(L,t) = \frac{dV(t)}{dt} = \frac{d}{dt}[(\theta^*(t) - \theta_n)L(t)] \tag{6}$$

In the mean time, the generalized Darcy's law for unsaturated flow is

$$q = - K(\psi)[(\partial\psi/\partial z) - 1] = K(\psi) - K(\psi)[(\partial\psi/\partial z)] \tag{7}$$

where ψ is the capillary potential (absolute value of the tension head), $K(\psi)$ is the unsaturated permeability. Integrating the above Eq. (7) from $z=0$ to $z=L_f(t)$, we introduce the average moisture flux q^*.

$$q^*(t)L = \int_0^{L_f(t)} K(\psi)\,dz - \int_0^{L_f(t)} K(\psi)\frac{\partial \psi}{\partial z}\,dz \tag{8}$$

For the analysis, the following hydraulic relations on unsaturated soil are adopted, ignoring the hysteresis effect.

$$K(\psi)/Ks = \{\psi_w/\psi\}^{\eta} \tag{9}$$

$$Se = (\theta - \theta_r)/(\theta_s - \theta_r) = \{\psi_w/\psi\}^{\beta} \tag{10}$$

where ψ_w is the air entry value, $K(\psi)$ and Ks are the permeabilities for unsaturated and saturated conditions, respectively. Se is the effective saturation, θ_s and θ_r are the volumetric moisture contents for saturated and for the case $K \to 0$, respectively. η and β are constants. From Eqs. (9) and (10), the relationship between K and Se is derived as

$$K(\psi)/Ks = Se^{\eta/b} \tag{11}$$

According to Brooks & Corey (1966), η and β are mutually related by the following equation.

$$\eta = 2 + 3\beta \tag{12}$$

Using Eqs. (9) and (10), the second term in right hand side of Eq. (8) is rewritten in the form

$$\int_0^{L_f(t)} K(\psi)\frac{\partial \psi}{\partial z}dz = Ks(-\psi_w)^{\eta}\int_0^{L_f(t)} \psi^{-\eta}d\psi$$

$$= \frac{-\psi_w}{\eta - 1}\left[K(0,t)Se(0,t)^{-1/\beta} - K(L_f,t)Se(L_f,t)^{-1/\beta}\right] \tag{13}$$

Substituting Eq. (13) to Eq. (8), we obtain the following expression of equivalent flux q^*.

$$q^*(t) = K^* + \frac{\psi_w}{\eta - 1}\cdot\frac{K^*Se^{*-1/\beta} - K_n\,Se_n^{-1/\beta}}{L} \tag{14}$$

where K^*, Se^* and K_n, Se_n are K, Se-values for θ^* and θ_n, respectively. Since the moisture in the zone below the position $z=L$ corresponds to the gravitational drainage condition, the moisture flux is represented as follows.

$$q(L,t) = K_n \tag{15}$$

Infiltration Process for constant rainfall intensity

In the case that the rainfall intensity Ra is constant in time and smaller than the saturated permeability Ks, a constant flux q_0 equal to Ra infiltrates from the ground surface. In this

state, since condition: $q^*=q_0$ is realized, Eq. (5) is rewritten as follows from Eqs. (6) and (15).

$$V(t) = (q_0 - K_n)t = [\theta^* - \theta_n]L(t) \tag{16}$$

The above equation is rewritten for $L(t)$ and substituted into Eq. (14). Ignoring infinitesimal terms by the conditions: $Se_n \ll 1$ and $K_n/q_0 \ll 1$, the following equation is then obtained.

$$q_0 = K^* + \frac{\psi_w(\theta_s - \theta_r)}{(\eta - 1)q_0 t} \cdot K^{*1-(1-\beta)/\eta} \cdot Ks^{(1-\beta)/\eta} \tag{17}$$

That is,

$$t = \frac{\psi_w(\theta_s - \theta_r)}{(\eta - 1)q_0(q_0 - K^*)} \cdot K^{*1-(1-\beta)/\eta} \cdot Ks^{(1-\beta)/\eta} \tag{18}$$

Based on the above equation, we can obtain the expression of the permeability K^* for the saturation of the equivalent moisture profile in any time. The equivalent moisture content θ^* and the depth of wetting front L are calculated from the following equations.

$$\theta^* = (\theta_s - \theta_r) \cdot (K^*/Ks)^{\beta/\eta} + \theta_r \tag{19}$$

$$L = V(t)/(\theta^* - \theta_n) = q_0 \cdot t/(\theta^* - \theta_n) \tag{20}$$

Redistribution Process after Rainfall

Since the volume of rain-water which infiltrates from the ground surface in a rainfall duration tr is $q_0 \cdot$ tr, the moisture volume $V(t)$ in soil after rainfall is

$$V(t) = q_0 \cdot tr - K_n \cdot t \tag{21}$$

The following expression should hold for $q(0,t)=0$ in the equation of continuity (6).

$$-L\frac{d\theta^*}{dt} = (\theta^* - \theta_n)\frac{dL}{dt} + K_n \tag{22}$$

The left hand side of this equation represents the decrease of moisture in the zone from the ground surface to the wetting front, and the right hand side the gravitational drainage and the downward seepage moisture accompanying the advance of the wetting front. Therefore, the downward moisture flux at the front may be evaluated by the following equation.

$$q^*(t) = -L\frac{d\theta^*}{dt} = \frac{-V(t)}{(\theta^* - \theta_n)}\frac{d\theta}{dt} \tag{23}$$

On the other hand, since the average moisture flux $q^*(t)$ has been given by Eq. (14), the following relation is derived from Eqs. (19)-(21) and the condition: $Se_n \ll 1$ and $(K_n/Ks) \ll 1$.

$$\frac{dK^*}{dt} = -\alpha \cdot K^{*2} \tag{24}$$

where

$$\alpha = \frac{\eta}{\beta q\, tr}\left[1 + \frac{\psi_w(\theta_s - \theta_r)}{(\eta - 1)q_0\, tr}(K^*/Ks)^{(\beta-1)/\eta}\right] \tag{25}$$

From the relation (12) between β and η, value of $(\beta-1)/\eta$ is -0.2 to 0.2 because value of β is usually 0.3 to 5.0. Therefore, the fluctuation of α is estimated small even if K^* changes largely, and α may be regarded as almost a constant. Solving Eq. (24) under the following initial condition (26), $K^*(t)$ is obtained as Eq. (27).

$$K^* = Ko : t = tr \tag{26}$$

$$K^*(t) = \frac{Ko}{1 + \alpha\, Ko(t - tr)} \tag{27}$$

where Ko is given as K^* by substituting $t=tr$ into Eq. (18). For the equivalent permeability K^* for θ^* in any time after rainfall is obtained by the above equation, the moisture profile, θ^* and L, can be calculated from Eqs. (19) and (20) by using the value of K^*.

Recharge Intensity to Aquifer

Let us consider about the recharge intensity to groundwater-table based on the approximate solution as obtained above. As well known, the unsaturated zone above water-table is composed of the capillary zone and the suspended water zone, and the recharge due to rainfall is caused when the vertical seepage water reaches at the top of the capillary zone. From this fact, the recharge intensity may be obtained by the following equation of water balance from the ground surface to the top of the capillary zone, $D'(t)$.

$$q(0,t) - q(D',t) = \frac{1}{\Delta t}\left[\int_0^{D'(t+\Delta t)} (\theta(z,t+\Delta t) - \theta_n)dz - \int_0^{D'(t)} (\theta(z,t) - \theta_n)dz\right] \tag{28}$$

where $q(0,t)$ and $q(D',t)$ are correspond to $Ra(t)$ and $Re(t)$, respectively. In this chapter, because the rising height of water-table is assumed to be small in comparison with the total length of the unsaturated zone, $D'(t)$ may be approximately regarded as a constant D'. Therefore, the above equation is simplified for the equivalent moisture profile.

$$Re(t) = Ra(t) + \frac{D'}{\Delta t}[\theta^*(t) - \theta^*(t+\Delta t)] \tag{29}$$

In the redistribution process in the situation of $Ra(t)=0$, the recharge volume in time interval Δt corresponds to the hatched part in Fig. 3. 4.

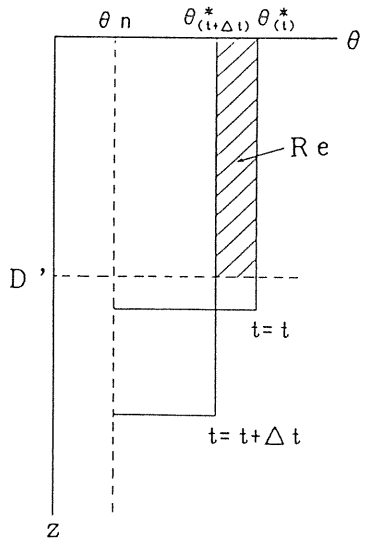

Fig. 3. 4 Recharge intensity to aquifer during redistribution process.

3. 2. 2 Verification of Approximate Model for Recharge Intensity

In this section, validity of the approximate recharge model is examined by comparison with the results of the numerical analysis based on the Richards' equation. The Richards' equation is given as follows from Eqs. (3) and (7).

$$\frac{\partial\theta(z,t)}{\partial t} = \frac{\partial}{\partial z}[K(\psi)\frac{\partial\psi}{\partial z}] - \frac{\partial K}{\partial z} \tag{30}$$

Eqs. (9)-(12) are used as the relationships among K, ψ and θ, and the following initial and boundary conditions are considered.

$$\theta(z,0) = \theta_n$$

$$q(0,t) = Ra\,(=\text{const.}) : \quad 0 < t \leqq tr$$

$$q(0,t) = 0 \qquad\qquad : \quad t > tr$$

Table 3. 1 Values of parameters in the analysis.

R a= 50 mm/hr β = 0. 3	t r= 2. 0 hr ψ w= 40 cm	D '= 160 cm θ s= 0. 2
CASE-1 K s=0. 002 cm/sec	θ n= 0. 09	θ r= 0. 08
CASE-2 K s= 0. 02 cm/sec	θ n= 0. 07	θ r= 0. 06

Two examples of $Re_0(t)$ are calculated for a fine soil (CASE-1) and for a coarse sand (CASE-2) as shown in Table 3.1. The calculations are carried out through the finite difference method as Δt=1sec and Δz=5cm. Fig. 3.5 shows the comparison of the moisture profiles for CASE-1 between (a) the numerical results and (b) the approximate analysis. From these figures, it is recognized that though the shape of the wetting front in (a) is smoothed due to the moisture diffusion effect, while the shape in (b) looks like steps. Of course, this difference is resulted from introducing the concept of the equivalent moisture profile in the approximate model. The recharge intensity $Re_0(t)$ for CASE-1 and CASE-2 are shown in Fig. 3. 6. In this figure, the solid and the broken lines show the approximate analysis and the numerical results, respectively. It is recognized that the recession curves of Re_0 are fitted sufficiently in both two cases, though the peak values of Re_0 are different largely each other. The difference between the peak values of numerical and approximated curves may be important in the discussion for the temporaly behavior of $Re_0(t)$. However, since these difference are similar to each other in two soil cases, they are no problem to discuss how the recharge process differs relatively due to the geology.

3. 2. 3 Spatial Distribution of Recharge due to Heterogeneity of Soil

In the previous section, the approximate model of the recharge intensity $Re_0(t)$ through the homogeneous soil has been formulated as the preparation for the discussion of the recharge through the heterogeneous soil. Let us consider then how the recharge intensity $Re(x,y,t)$ varies by the horizontal nonuniformity of hydraulic properties in unsaturated zone, on the basis of the approximate model. Here, both the log-saturated permeability $Y(x,y)=ln[Ks(x,y)]$ and the effective porosity $Pe(x,y)=\theta_s-\theta_r$ are assumed to follow the normal distribution. It is also assumed that the rainfall intensity Ra and the period of rainfall duration tr are constants, and the other factors such as β,η and ψ_w etc. are deterministic values that depend on the average properties in unsaturated soil, respectively. Moreover, we will write $Y(x,y)$ and $Pe(x,y)$ as the summation of the average quantities (Y_0 and Pe_0) and the small variations (Y_1 and Pe_1).

$$Y(x,y) = Y_0 + Y_1(x,y)\,, \quad |Y_0| \gg |Y_1| \tag{31a}$$

$$Pe(x,y) = Pe_0 + Pe_1(x,y)\,, \quad |Pe_0| \gg |Pe_1| \tag{31b}$$

As stated in the previous section 3.1, $Re(x,y,t)$ consists of the spatial average $Re_0(t)$ and the small fluctuation $Re_1(x,y,t)$, that is,

$$Re(x,y,t) = Re_0(t) + Re_1(x,y,t) \tag{32}$$

The recharge intensity during the redistribution process in unsaturated zone is obtained as follows by substituting Eqs. (19) (27) into Eq.(29).

$$Re(x,y,t) = \frac{D'\cdot Pe(x,y)}{\Delta t\cdot Ks(x,y)^{\beta/\eta}} \cdot \left[\left(\frac{Ko}{1+\alpha Ko(t-tr)}\right)^{\beta/\eta} - \left(\frac{Ko}{1+\alpha Ko(t+\Delta t-tr)}\right)^{\beta/\eta}\right] \tag{33}$$

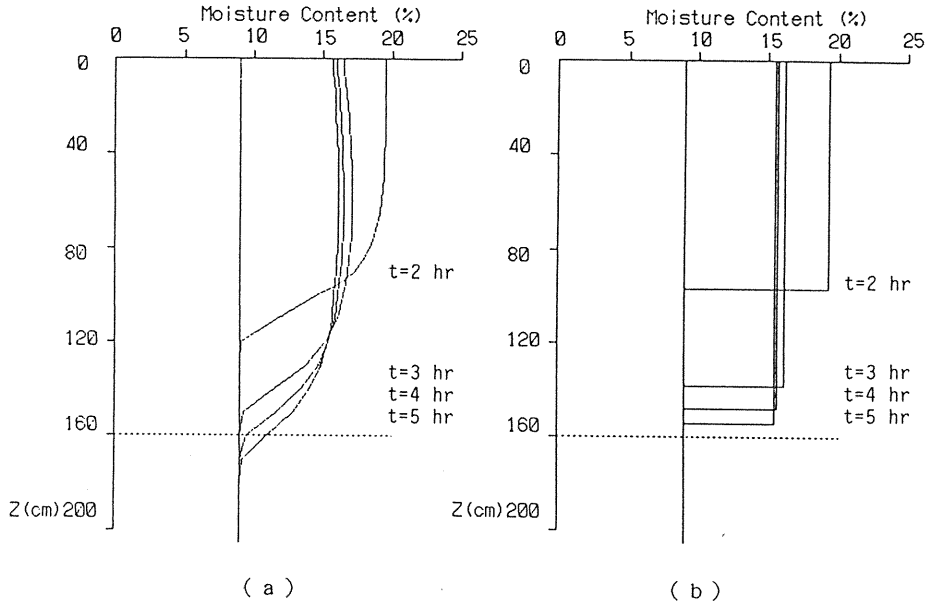

Fig. 3. 5 Comparison of moisture profiles: (a) numerical results, (b) approximate analyses.

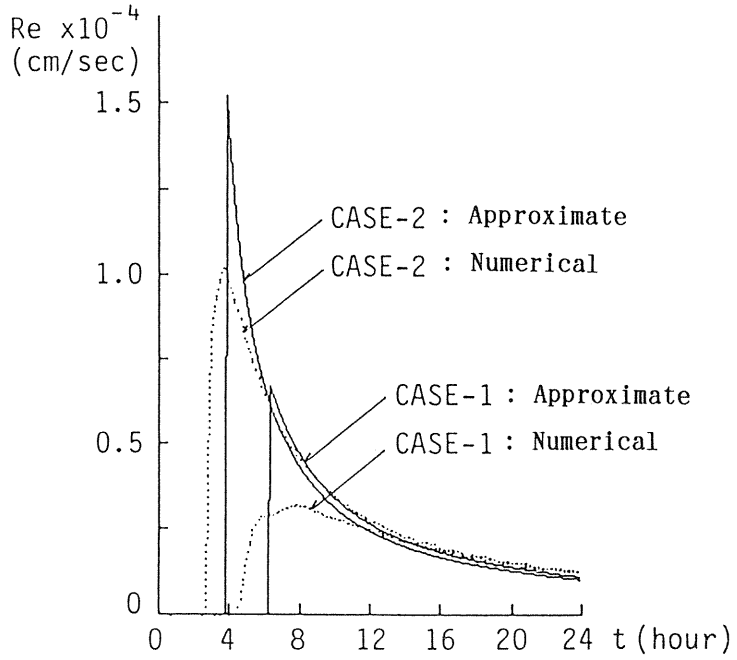

Fig. 3. 6 Comparison of recharge intensity: (solid lines) approximate analyses, (broken lines) numerical results.
CASE-1: a fine soil, CASE-2: a coarse sand

where Ko and α are given by Eqs. (18) and (25), respectively. Both of these equations involve the $(\beta-1)/\eta$ th power of $Pe(x,y)$ and $Ks(x,y)$. According to Eq.(12), since both $(\beta-1)/\eta$ and β/η are small values that nearly equal to zero, the part of the bracket [ ] in the above equation can be regarded approximately as constant for $Ks(x,y)$ and $Pe(x,y)$, that is,

$$Re(x,y,t) = A(t)\frac{Pe(x,y)}{Ks(x,y)^{\beta/\eta}} \tag{34}$$

This equation is combined with Eq. (31a) into

$$Ks(x,y)^{\beta/\eta} = \exp[(\beta/\eta)(Y_0 + Y_1(x,y))]$$

$$= Ks_0^{\beta/\eta}[1 + \frac{\beta}{\eta}Y_1 + \frac{1}{2!}(\frac{\beta}{\eta}Y_1)^2 + \cdots] \tag{35}$$

Substituting Eqs. (31b) (32) (35) into Eq. (34) and ignoring infinitesimal terms, the fluctuation of $Re(x,y,t)$ may be expressed as

$$Re(x,y,t) = A(t)\frac{Pe_0}{Ks_0^{\beta/\eta}}[1 + \frac{Pe_1(x,y)}{Pe_0} - \frac{\beta}{\eta}Y_1(x,y)] \tag{36}$$

On the other hand, from Eq. (34),

$$Re(x,y,t) = A(t)\frac{Pe_0}{Ks_0^{\beta/\eta}} \tag{37}$$

$Re_1(x,y,t)$ and $Re(x,y,t)$ may be, then, finally formulated in the following form.

$$Re_1(x,y,t) = C(x,y)\ Re_0(t) \tag{38}$$

$$Re(x,y,t) = (1 + C(x,y))\ Re_0(t) \tag{39}$$

where $$C(x,y) = Pe_1(x,y)/Pe_0 - (\beta/\eta)Y_1(x,y) \tag{40}$$

The variance of $Re(x,y,t)$ may be also given as follows.

$$\sigma_{Re}^2(t) = E[C(x,y)^2]Re_0(t)^2 \tag{41}$$

The equations obtained above is what give the spatial distribution of the recharge to the groundwater-table resulted from the horizontal heterogeneity of geology in the region concerned.

3. 3 Stochastic Head Response Process in Heterogeneous Aquifer

3. 3. 1 Random Component of Head Behavior

With respect to the head rising process in unconfined aquifer, the stochastic characteristics of the random head response to the spatial fluctuation of $Re(x,y,t)$ is discussed here from

physical view point, that is, by means of the groundwater flow equation. The linearization in terms of the effective thickness H_0 (constant) of aquifer leads the following two dimensional fundamental equation of the unconfined groundwater flow on the horizontal impermeable base.

$$S(x,y)\frac{\partial h}{\partial t} = \frac{\partial}{\partial x}[Ks(x,y)H_0\frac{\partial h}{\partial x}] + \frac{\partial}{\partial y}[Ks(x,y)H_0\frac{\partial h}{\partial y}] + Re(x,y,t) \tag{42}$$

where $h(x,y,t) = H^*(x,y,t) - H_0$, $H^*(x,y,t)$ is the water depth and $|H_0| \gg |h(x,y,t)|$. $Ks(x,y)$ and $S(x,y)$ are the saturated permeability and the specific yield in the aquifer, respectively. Although $S(x,y)$ corresponds physically to the effective porosity $Pe(x,y)$ in unsaturated soil, $S(x,y)$ and $Pe(x,y)$ are distinguished each other in this section, because they express the characteristics of different zones, that is, in the aquifer and in the unsaturated zone. We shall assume that the flow domain is gradually heterogeneous and $Y(x,y)$, $S(x,y)$ can be decomposed into their averages (Y_0 and S_0) and the small variantions (Y_1 and S_1).

$$Y(x,y) = Y_0 + Y_1(x,y)\,, \quad |Y_0| \gg |Y_1| \tag{43a}$$

$$S(x,y) = S_0 + S_1(x,y)\,, \quad |S_0| \gg |S_1| \tag{43b}$$

Moreover, assuming that $h(x,y,t)$ varies a little in the neighborhood of the head h_0, which will appear in the homogeneous region with geological characteristics Y_0 and S_0, the following relation is obtained.

$$h(x,y,t) = h_0(x,y,t) + h_1(x,y,t), \quad E[h(x,y,t)] = h_0(x,y,t) \tag{44}$$

As will be easily understood, the quantity h_1 is the head deviation caused by the geological heterogeneity of the aquifer and the spatial deviation of the recharge $Re(x,y,t)$. These relations (40) (43) and (44) are substituted into Eq. (42). Moveover, considering that the flow in the homogeneous aquifer is governed by the following Eq. (45) and ignoring higher-order terms, we obtain Eq. (46).

$$S_0\frac{\partial h_0}{\partial t} = Ks_0H_0\frac{\partial^2 h_0}{\partial x^2} + Ks_0H_0\frac{\partial^2 h_0}{\partial y^2} + Re_0(t) \tag{45}$$

$$\begin{aligned}\frac{S_0}{Ks_0H_0}\frac{\partial h_1}{\partial t} - \frac{\partial^2 h_1}{\partial x^2} - \frac{\partial^2 h_1}{\partial y^2} - \frac{Re_0(t)}{Ks_0H_0}\cdot C(x,y) \\ = -\frac{S_1(x,y)}{S_0}[\frac{\partial^2 h_0}{\partial x^2} + Ks_0H_0\frac{\partial^2 h_0}{\partial y^2} + \frac{Re_0(t)}{Ks_0H_0}] \\ + \frac{\partial}{\partial x}[Y_1(x,y)\frac{\partial h}{\partial x}] + \frac{\partial}{\partial y}[Y_1(x,y)\frac{\partial h}{\partial y}]\end{aligned} \tag{46}$$

For the sake of simplification, assume that the head-field before rainfall is sufficiently calm and the initial distribution is horizontally flat, that is, $h(x,y,0)$=const. In this case, since the distribution of head rising height due to $Re_0(t)$ becomes also constant spatially, the above equation is rewritten as follows.

$$\frac{S_0}{Ks_0H_0}\frac{\partial h_1}{\partial t}-\frac{\partial^2 h_1}{\partial x^2}-\frac{\partial^2 h_1}{\partial y^2}=\frac{Re_0(t)}{Ks_0H_0}[C(x,y)-\frac{S_1(x,y)}{S_0}] \tag{47}$$

Considering an infinite domain as the analysis region and solving the equation under the initial conditions $h_0(x,y,0)$=const. and $h_1(x,y,0)$=0, the random component of head, $h_1(x,y,t)$ is obtained as follows.

$$h_1(x,y,t)=\frac{Ks_0H_0}{S_0}\int_0^t dt'\iint_{-\infty}^{\infty} dx'dy'\,G(x,x',y,y',t-t')\,U(x',y',t') \tag{48}$$

where

$$U(x,y,t)=\frac{Re_0(t)}{Ks_0H_0}[C(x,y)-\frac{S_1(x,y)}{S_0}] \tag{49}$$

$G(x,y,t)$ is the Green function for the two dimensional diffusion equation.

3. 3. 2 Statistical Variance of Head Response

The statistical variance which represents the spatial randomness of head-field, namely "head variance", is written as follows, on the basis of the weakly stationary hypothesis.

$$\begin{aligned}\sigma_h^2 &= Var[h(x,y,t)]=E[h_1(x,y,t)^2]\\ &=[\frac{Ks_0H_0}{S_0}]^2\iint_0^t dt'dt''\iiint\!\!\iint_{-\infty}^{\infty} dx'dx''dy'dy''\\ &\cdot G(x,y,x',y',t-t')G(x,y,x'',y'',t-t'')]\;E[U(x',y',t')U(x'',y'',t'')]\end{aligned} \tag{50}$$

Provided the spatial correlation of $C(x,y)$ and $S_1(x,y)$ can be approximated as it of the "white noise process", the covariance of $U(x,y,t)$ in the above equation is replaced as follows in terms of the Dirac's delta function.

$$E[U(x',y',t')U(x'',y'',t'')]=\frac{Re_0(t')Re_0(t'')}{(Ks_0H_0)^2}\sigma_{CS}^2\rho_0^2\delta(x''-x')\delta(y''-y') \tag{51}$$

in which

$$\sigma_{CS}^2=Var[C(x,y)-\frac{S_1(x,y)}{S_0}] \tag{52}$$

$\delta(\cdot)$ denotes the Dirac's delta function, and ρ_0 is a constant on the white noise assumption of $U(x,y,t)$. From Eqs. (50) (51) and (52), we obtain

$$\sigma_h^2(t)=\frac{\sigma_{CS}^2\cdot\rho_0^2}{4\pi\cdot Ks_0H_0\cdot S_0}\int_0^t\int_0^t\frac{Re_0(t')Re_0(t'')}{2t-t'-t''}dt'dt'' \tag{53}$$

where σ_{CS}^2 is summation of the variances of $C(x,y)$ and $S(x,y)$: For the case that Pe_1, Y_1 and S_1 are mutually independent, σ_{CS}^2 becomes

$$\sigma_{CS}^2 = [\frac{1}{Pe_0^2}]\sigma_P^2 + [\frac{\beta^2}{\eta^2}]\sigma_Y^2 + [\frac{1}{S_0^2}]\sigma_S^2 \tag{54}$$

in which σ_P^2, σ_Y^2 and σ_S^2 are the variances of $Pe(x,y)$, $Y(x,y)$ and $S_1(x,y)/S_0$, respectively. This is the equation which expresses the stochastic property σ_h^2 of head rising due to a rainfall, caused by the heterogeneity in both of the unsaturated zone and the aquifer.

Examples of the head variance calculated by Eq. (53) are shown in Fig. 3. 7 with solid lines. In the figure, the same Re_0(t) shown in Fig. 3. 6 are also drawn once more with broken lines. CASE-1 and CASE-2 in the figure correspond to the cases of a fine soil and a coarse sand, respectively. According to this figure, the difference between the variances of CASE-1 and CASE-2 attracts our attention. Although CASE-2 is larger than CASE-1 in their peak values of $Re_0(t)$, the head variance for CASE-1 is estimated far larger than CASE-2. That is, $Re_0(t)$ and $\sigma_h^2(t)$ behave oppositely in the figure. This result suggests that the variance of head response to rainfall is governed in rather complex way by both of the transformation from the rainfall *Ra* to the recharge *Re* in the unsaturated zone and the transformation from *Re* to the head behavior in the aquifer.

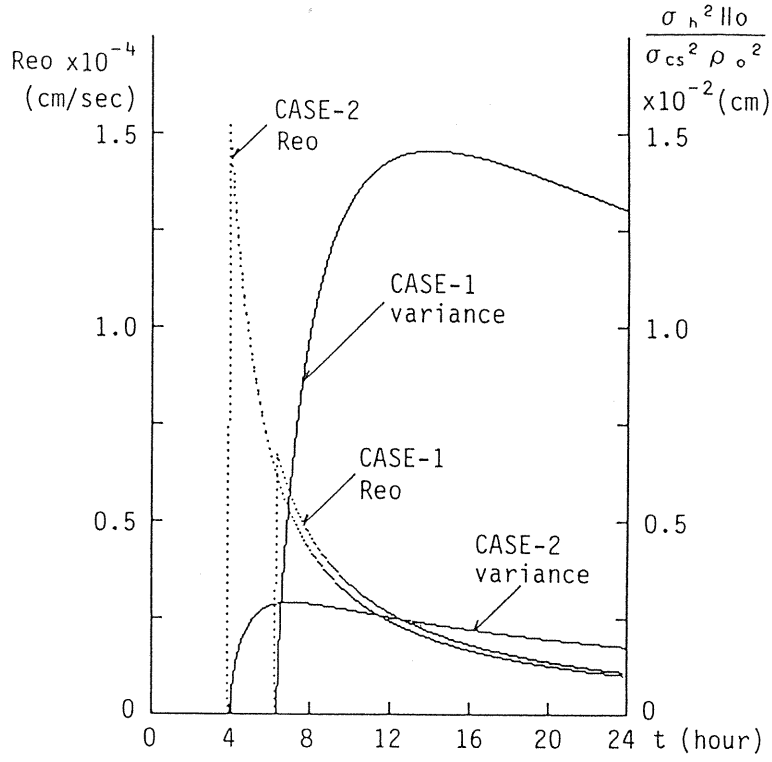

Fig. 3. 7 Examples of recharge intensity and head variance.
CASE-1: a fine soil, CASE-2: a coarse sand

3. 3. 3 *Uncertainties of Head Response under Various Geology*

On the basis of the results as stated above, we will discuss what kind of the geological condition makes the head response random. For that, three average values of the hydraulic properties in the flow domain; the permeability Ks_0, the effective porosity Pe_0 in soil and the specific yield S_0, are adopted as the geological condition which affects on the head response.

Relationship between Recharge Intensity and Hydraulic Properties

As seen from Eq. (53), the head variance involves the integral of the average recharge intensity $Re_0(t)$. Then, at first the relationship between $Re_0(t)$ and the average hydraulic properties (Ks_0, Pe_0) is calculated as shown in Fig. 3. 8. The figure indicates the logarithm of the maximum value of $Re_0(t)$ for various pairs of Ks_0 and Pe_0. In calculation of this figure, the other factors except Ks_0 and Pe_0 are given as shown in Table 3. 2. According to the distribution of values in the figure, it is recognized that $Re_0(t)$ takes the larger value in the case with larger Ks_0 and smaller Pe_0. Two solid curves in the figure are drawn by Eq. (37), that is,

$$\frac{Re_0(t)}{A(t)} = \frac{Pe_0}{Ks_0^{\beta/\eta}} \tag{55}$$

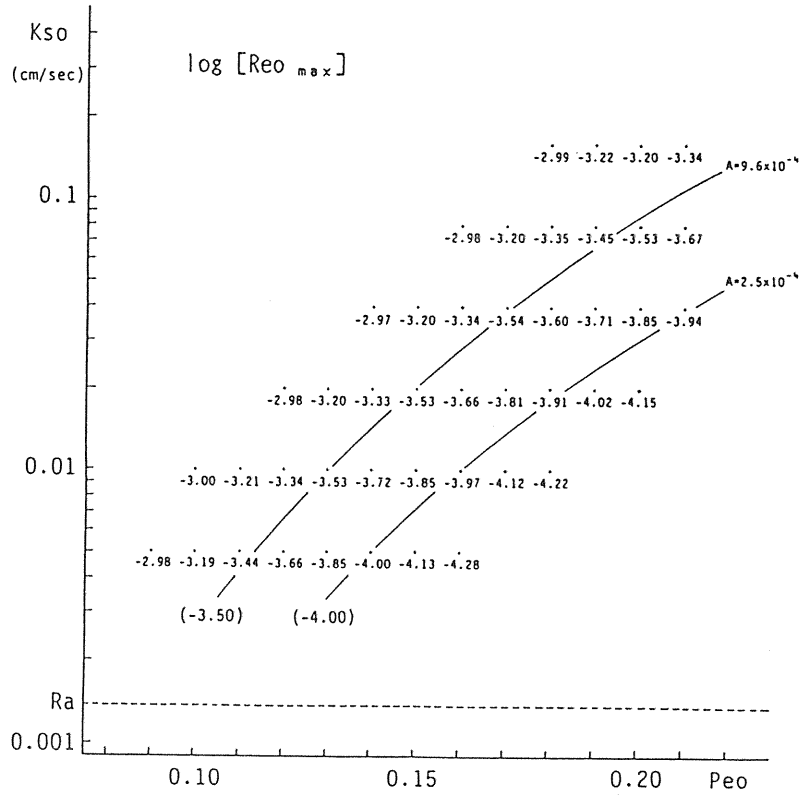

Fig. 3. 8 Relationships between recharge intensity and hydraulic properties in unsaturated soil.

Table 3. 2 Values of parameters in the analysis.

Ra= 50 mm/hr	tr= 2.0 hr	D' = 160 cm
β = 1.0	ϕ w= 40 cm	(η = 5.0)

From the good fitting between the curves and the values, the curves may be regarded as the contour lines of log[$Re_0(t)$]. This fact means that the value of the left hand side in Eq. (55) becomes constant for various values of Ks_0 and Pe_0 on the curve. In other words, among the various soils which have different properties of (Ks_0, Pe_0) on the same curve, $I = Pe_0 / Ks_0^{\beta/\eta}$ remains at a constant value, and the groundwater recharge takes place with same intensity by counteracting both differences of the permeability and the storativity of water. Therefore, the above ratio I may be considered as an index that expresses the superiority of the hydraulic properties in soil.

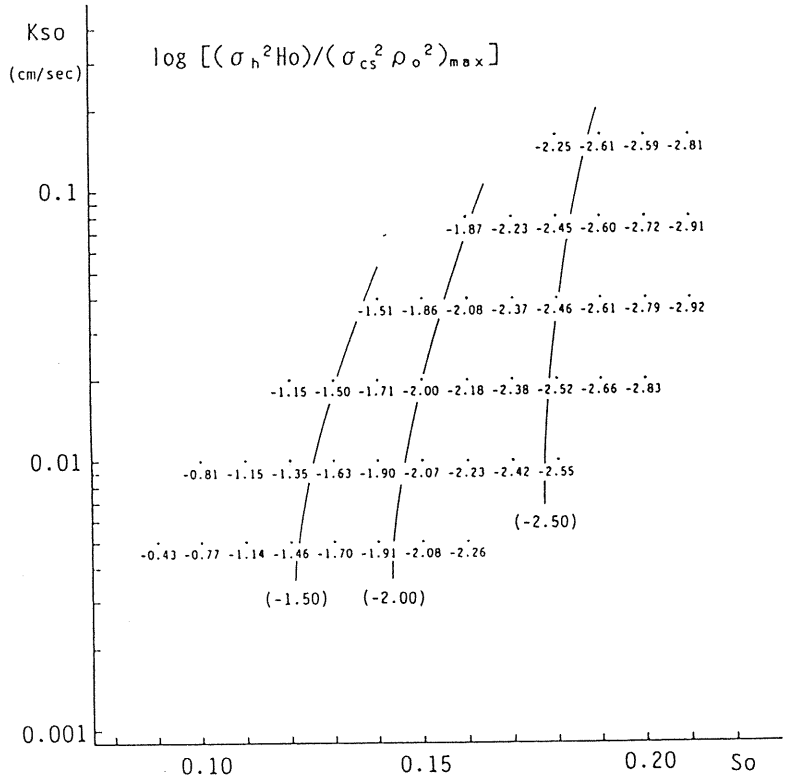

Fig. 3. 9 Relationships between head variance and hydraulic properties in aquifer.

Relationship between Head Variance and Hydraulic Properties

Let us see the influence of the average hydraulic properties to the head variance, for the same case of Fig. 3. 8. The logarithm of the maximum values of head variance $(\sigma_h^2 H_0)/(\sigma_{CS}^2 \rho_0^2)$ are shown for various pairs of (Ks_0, S_0) in Fig. 3. 9. Solid curves in the figure represent contour lines of the head variance. These curves have more steep gradients than those in Fig. 3. 8. If we try to put Fig. 3. 8 on Fig. 3. 9 because Pe_0 and S_0 are physically same each other, it is resulted that the head variances are considerably different according to the kinds of soils, even though the regions have the same recharge intensity Re_0. That is, the head variance becomes large in a fine soil of which Ks_0 and S_0 are relatively small, and becomes small in a coarse sand. This fact means that the head-field is more apt to be disturbed by rainfall in a aquifer that consists of coarse sand and gravel, such as in the alluvial fan, than in a aquifer that consists of silt and fine sand, such as in diluvial terras. This result implies also that the observation of head and the evaluation of data should be changed according to the properties of objective aquifer.

4. Stochastic Analysis of Recession Process of Head-Field after Rainfall

4. 1 Uncertainty of Head-Field in Recession Process and Its Evaluation

In previous chapter, the head variance of the rising process has been formulated by regarding the distribution of head rising in a heterogeneous region as the physical phenomena in a stochastic random field. In the flow region where the distributions of hydraulic properties have little spatial correlation, the head response process is also spatially independent, because the phenomena take place within a short term. Therefore it is sufficient for statistical expression of the head-field to evaluate the average and the variance. However, in the head recession process during a dry period after rainfall, local components of head fluctuation are reduced by the lateral flow in aquifer, and the head behavior with regional scale governed by the aquifer structure and the boundary conditions come in sight. In other words, randomness and spatial correlation of the head-field change obviously with the passage of time. In this chapter, we will discuss the unsteady head variogram as a quantitative concept expressing the spatial statistical structure of the head-field. That is, the variogram is defined as the following equation for the random head component $h_1(\mathbf{X}, t)$ due to the heterogeneity of aquifer.

$$\gamma(d,t) = \frac{1}{2} E[\{h_1(\mathbf{X}+\mathbf{d},t) - h_1(\mathbf{X},t)\}^2] \tag{56}$$

where $\mathbf{X}$: the location vector, t: time, $d=|\mathbf{d}|$: the distance between two points in the region concerned, moreover $E[\cdot]$ denotes the statistical expectation.

By the way, as mentioned at the beginning of this paper, the analysis of regional groundwater is accompanied with some uncertainties caused by insufficiency of the observation information in addition to complexity of the phenomena. Especially, since the observed data of head are given only at a limited set of well points, it is necessary for the evaluation of spatial distribution of head to interpolate rationally the head states at non-observed points from their point data. The traditional contour mapping by hand drawing as a interpolation method depends on subjectivity even in case of smooth distribution, much more in case that the head behaves randomly in heterogeneous aquifer. Although some methods for automatic mapping have been developed to avoid the subjectivity, many of them neither treat physical properties

of the phenomena nor indicate accuracy of the estimated results. To overcome week points of these conventional methods, "kriging" has been created by Matheron and his group (Journel & Huijbregts, 1978; Delhomme, 1978). Kriging is an estimation method of the random field from a limited set of observed values based on the geostatistic approach, and is able to indicate also the estimation accuracy as "kriging error" besides the estimated values through the variogram $\gamma(d)$ and the drift function of the variable concerned. In the latter part of this chapter, applicability of kriging to the head-field in the actual aquifer will be discussed by using the head variogram derived analytically.

4. 2 Spatial Structure of Head-Field during Recession Process

4. 2. 1 Random Component of Head Behavior

If the linearization using the effective thickness H_0 (constant) of aquifer is possible, two dimensional fundamental equation of the unconfined groundwater flow on the horizontal base takes the following form,

$$S(x,y)\frac{\partial h}{\partial t}=\frac{\partial}{\partial x}[K(x,y)H_0\frac{\partial h}{\partial x}]+\frac{\partial}{\partial y}[K(x,y)H_0\frac{\partial h}{\partial y}] \tag{57}$$

where $h(x,y,t) = H^*(x,y,t) - H_0$, $H^*(x,y,t)$ is the water depth on the impermeable base and $|H_0| \gg |h(x,y,t)|$. $S(x,y)$ and $K(x,y)$ are the effective porosity and the permeability in the aquifer, respectively. We assume that the flow domain is gradually heterogeneous, and that $S(x,y)$ and log-transmissivity $Y(x,y)$ defined as $ln[K(x,y)H_0]$ can be decomposed into the quantities (S_0 and Y_0) in averaged homogeneous region and the small variations (S' and Y') around them.

$$S(x,y) = S_0 + S'(x,y)\,, \quad |S_0| \gg |S'(x,y)| \tag{58a}$$

$$Y(x,y) = Y_0 + Y'(x,y)\,, \quad |Y_0| \gg |Y'(x,y)| \tag{58b}$$

Similarly, assuming that $h(x,y,t)$ in the heterogeneous region varies a little in the neighborhood of the head $h_0(x,y,t)$ in the averaged homogeneous region, we write

$$h(x,y,t) = h_0(x,y,t) + h_1(x,y,t) \tag{59}$$

Substituting these relations (58) and (59) into Eq. (57) and ignoring the higher-order infinitesimals, we obtain

$$\frac{S_0}{e^{Y_0}}\frac{\partial h_1(x,y,t)}{\partial t}-\frac{\partial^2 h_1(x,y,t)}{\partial x^2}-\frac{\partial^2 h_1(x,y,t)}{\partial y^2}=g(x,y,t) \tag{60}$$

in which

$$g(x,y,t)=\frac{S'(x,y)}{e^{Y_0}}\frac{\partial h_0(x,y,t)}{\partial t}+\frac{\partial}{\partial x}[Y'\frac{\partial h_0(x,y,t)}{\partial x}]+\frac{\partial}{\partial y}[Y'\frac{\partial h_0(x,y,t)}{\partial y}]$$

Let us consider an infinite domain as the region concerned. Provided the initial condition $h_1(x,y,0) = \phi_1(x,y)$ is given, the first-order solution for h_1 is obtained as

$$h_1(x,y,t) = \int_{-\infty}^{\infty}\int_{-\infty}^{\infty} G(x,y,x',y',t)\,\phi_1(x',y')dx'dy' + \lambda_0 \int_{-\infty}^{\infty}\int_{-\infty}^{\infty} G(x,y,x',y',t-\tau)\,g(x',y',\tau)dx'dy'd\tau \tag{61}$$

in which

$$G(x,y,x',y',t) = \frac{1}{4\pi\lambda_0 t}\exp[-\frac{(x-x')^2+(y-y')^2}{4\lambda_0 t}], \quad \lambda_0 = \frac{e^{Y_0}}{S_0}$$

This is the equation which represents the time evolution of the random component of head distribution due to the aquifer heterogeneity.

4. 2. 2 Theoretical Variogram of Unsteady Head-Field after Rainfall

Let us consider the unsteady process in which the random head distribution just after rainfall is gradually flattened during a long dry period. Dagan (1982) has discussed the head variogram based on the second term in the right hand side of Eq. (61) in the case that initial head is deterministically given, that is $\phi_1(x,y) = 0$. However, we neglect the second term because it seems that the role of this term is small in comparison with the first term, in the phenomena treated here. Hence, taking the lag-distance d in the x direction, the following head variogram may be derived from the above physical solution.

$$\gamma(d,t) = \frac{1}{2}E[\{h_1(x+d,y,t) - h_1(x,y,t)\}^2]$$
$$= \int_{-\infty}^{\infty}\int_{-\infty}^{\infty} dx'dy' \int_{-\infty}^{\infty}\int_{-\infty}^{\infty} dx''dy'' \{[G(x,y,x',y',t)G(x,y,x'',y'',t) - G(x+d,y,x',y',t)G(x,y,x'',y'',t)]\,E[\phi_1(x',y')\,\phi_1(x'',y'')]\} \tag{62}$$

By defining the autocorrelation function ρ_ϕ and the variance σ_ϕ^2 of the random component $\phi_1(x,y)$ in the initial head distribution, the covariance of $\phi_1(x,y)$ can be written by

$$E[\phi_1(x',y')\,\phi_1(x'',y'')] = \sigma_\phi^2\,\rho_\phi(x',y',x'',y'') \tag{63}$$

Provided $\phi_1(x,y)$ can be assumed to be the "white noise process", ρ_ϕ is represented as

$$\rho_\phi(x',y',x'',y'') = \rho_1\,\delta(x'-x'')\delta(y'-y'') \tag{64}$$

where $\delta(\cdot)$ denotes the Dirac's delta function and ρ_1 is a constant.
Substituting these relations (63) and (64) into Eq. (62) and carrying out the integration, finally we obtain the head variogram:

$$\gamma(d,t) = \sigma_h^2(t)\,[1 - \rho(d,t)] \tag{65}$$

where $\sigma_h^2(t) = \dfrac{\sigma_\phi^2 \rho_1}{8\pi\lambda_0 t}$, $\rho(d,t) = \exp(-\dfrac{d^2}{8\lambda_0 t})$

Since the head-field is assumed to be statistically isotropic, the variogram obtained above can be available for the lag d in any direction. In this way, we introduce the functional form of variogram based on the physical flow equation, which has been estimated statistically only by the observed data.

In Fig. 4. 1, the head variogram Eq. (65) is represented as dimensionless function of lag d for any time after a rainfall. In this figure, the variogram $\gamma(d,t)$ takes a form gradually approaching to a constant value with increasing of lag d. This constant value is usually called the 'sill' and the lag-distance which is needed for variogram to approach the sill is called the 'range'. The figure shows that the sill decreases rapidly and the range increases little by little with the passage of time. This means that the head-field after a rainfall smooths down with the reduction of the randomness and with the spreading of the spatial correlation scale due to the average diffusivity λ_0 of aquifer.

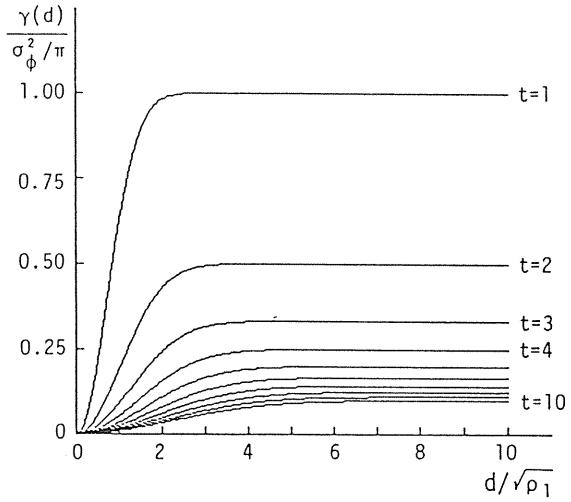

Fig. 4. 1 Theoretical head variogram in recession process ($\rho_1/(8\lambda_0) = 1.0$).

4. 3 Stochastic Estimation of Head-Field in Actual Region

4. 3. 1 Application of Universal Kriging and Its Problems

With help of the theoretical functional form of the variogram Eq. (65), we shall estimate the spatial distribution of head from a limited set of observed point data. If the complex behavior of head-field due to rainfall can be regarded as a probabilistic variable in two dimensional "random field", we can apply the kriging method to the objective estimation of the random field, based on the geostatistic approach. An outline of the kriging method, especially the universal kriging as a method for the non-stationary random field, is summarized as follows.

Let $Z(X)$ be a head value at a point X (X denotes the location vector). $Z(X)$ is defined as the sum of the drift or trend $m(X)$ and the residue $R(X)$ in Eq. (66), and $m(X)$ is assumed to be locally representable by polynomial expression in Eq. (67), that is,

$$Z(X) = m(X) + R(X) \tag{66}$$

$$E[Z(X)] = m(X) = \sum_{l}^{k} a_l f^l(X) \tag{67}$$

where $f^l(X)$ (l=1,2,$\cdots$,k) are polynomial functions, a_l(l=1,2,$\cdots$,k) are their coefficients, k is the number of drift terms. Between any points X_1 and X_2 with the distance d_{12}, the statistic function on $Z(X)$ is defined as

$$Var[Z(X_1) - Z(X_2)] = E[\{R(X_1) - R(X_2)\}^2] = 2\gamma(d_{12}) \tag{68}$$

where $d_{12} = |X_1 - X_2|$, the function $\gamma(d)$ is so-called 'semi-variogram' (for short, 'variogram') and represents the spatial correlation of the random process $Z(X)$. Universal kriging is developed as an estimation method of non-stationary random field from a limited set of observed values, through the functions $\gamma(d)$ and $m(X)$. The main idea of this method is to consider an observed value as a realization of random field. The optimum estimator $\hat{Z}(X)$ of unknown variable $Z(X)$ is obtained as the Best Linear Unbiased Estimator (BLUE), satisfied with

$$\hat{Z}(X) = \sum_{i}^{n} W_i Z_i \tag{69a}$$

$$Var[\hat{Z}(X) - Z(X)] \rightarrow \min. \tag{69b}$$

$$E[\hat{Z}(X) - Z(X)] = 0 \tag{69c}$$

where Z_i is the observed value at the point i(i=1,2,$\cdots$,n), W_i is the weighting coefficient corresponding to Z_i and the sum of W_i is 1.0. From the above conditions (69), the kriging equations (i=1,2,$\cdots$,n, l=1,2,$\cdots$,k) can be derived as the following equation estimating the unknown weighting coefficient W.

$$\sum_{j}^{n} W_j \gamma(d_{ij}) + \sum_{l}^{k} \mu_l f^l(X_i) = \gamma(d_i) \tag{70}$$

$$\sum_{i}^{n} W_i f^l(X_i) = f^l(X) \tag{71}$$

where $d_{ij} = |X_i - X_j|$, $d_i = |X - X_i|$, μ_l are the Lagrangian multipliers. By solving these equations, W_i and μ_l at any points are calculated, and then the BLUE $\hat{Z}(X)$ are found out. Kriging variance which expresses the estimation error of the head at any point can be also obtained by

$$Var[\hat{Z}(X) - Z(X)]_{\min.} = \sum_{i}^{n} W_i \gamma(d_i) + \sum_{l}^{k} \mu_l f^l(X) \tag{72}$$

For the application of universal kriging, the variogram $\gamma(d)$ and the number of drift terms k on $Z(X)$ should be given in advance. If the mean of $Z(X)$ is constant, namely 'no drift', it is usually not impossible to infer $\gamma(d)$ from observed data by assuming that $Z(X)$ is ergodic. However, in the non-stationary case, we cannot know both $\gamma(d)$ and $m(X)$ at once because the residue $R(X)$ is unknown. Even though $m(X)$ become a known function in some manners, it is required that a large number of observation points exist with the high spatial density, to find out the functional form of $\gamma(d)$ from $R(X)$ data. Considering the spatial sparseness of usual observatory network, it is very difficult to determine the statistic functions by using only the measured data. For the groundwater phenomena considered in this study, however, a functional form of the unsteady variogram $\gamma(d,t)$ on the head-field has been already derived from the flow equation analytically. Therefore, the following analysis procedures may be adopted to overcome the difficulty mentioned above. At first, both the drift function $m(X)$ is proposed as Eq. (67) and the number of drift terms k are decided by the multiple regression of data on $Z(X)$. The Ordinary Least Squares (OLS) cannot be used strictly in the regression analysis because the residue $R(X)$ has a spatial correlation generally. But, in this application, the OLS is adopted approximately by utilizing the roughness of observatory network. Secondly, the parameters of function $\gamma(d,t)$ are identified by means of the variance on $R(X)$ obtained by regression of the drift.

4. 3. 2 Identification of Number of Drift Terms and Variogram

Let us apply the kriging method to Basin B (Fig. 2. 3) stated in chapter 2. Kriging analysis is carried out at three time stages (ST. I, II, III) in Fig. 4. 2. These time stages represent

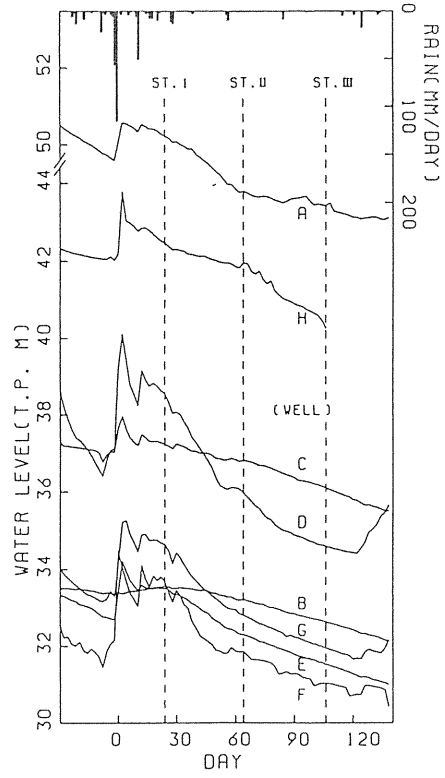

Fig. 4. 2 Fluctuations of observed heads (Sep. 1983—Feb. 1984).

the situations at 24, 64, 104 days after the storm rainfall in September 1983, respectively. As stated in section 4. 3. 1, it is necessary for application of kriging that the number of drift terms and parameters of the variogram are identified to adjust the fluctuation of natural phenomenon.

First, the parameters of drift $m(x)$ modeled by Eq. (67) were identified by the multiple regression analysis. The optimum number of terms k was decided based on AIC (Akaike Information Criterion, Akaike (1973)). As a result, the drift function (67) could be represented by 6 terms for this region, that is, quadratic drift, on any stages. Table 4. 1 shows the identified values of coefficient a_l and the residual variances.

Secondly, the parameters involved in $\gamma(d)$ can be identified as follows: As shown in Eq. (65), the variogram $\gamma(d)$ are composed of the head variance σ_h^2 and the autocorrelation function $\rho(d)$ of h_1. Since $\rho(d)$ depends on only average diffusivity λ_0 of aquifer, it is possible to evaluate the spatial correlation in $\gamma(d)$, if mean values of permeability and effective porosity are given in some manner. In this study region, the value of λ_0 was assumed to be $10(m^2/day)$ by judging the kind of geological deposit (Takagi & Harada, 1988).

Another factor σ_h^2 includes unknown parameters $\sigma_\phi^2\rho_1$ and λ_0. However, σ_h^2 can be identified in comparing with the residual variance obtained in the drift regression. Fig. 4. 3 shows comparison of the residual variances in Table 4. 1 with theoretical values of σ_h^2 in setting $\sigma_\phi^2\rho_1 = 3300(m^4)$. From the figure, we can recognize rough suitability of the formulation of head variance.

4. 3. 3 Universal Kriging of Head-Field

Kriging estimation is carried out by choosing 600 points in the entire region concerned, with an equal interval of 20 meters. Fig. 4. 4 illustrates the estimation result of hydraulic head-field at various time stages ST. I, II and III after rainfall, and Fig. 4. 5 shows the distribution of kriging deviation (square root of Eq. (72)) which corresponds to the estimation error at all points in Fig. 4. 4. These figures represent the most objective head-field and their confidence limit expected from the observed information at 8 wells. In Fig. 4. 4, we can recognize that the head-field distributes following the ground-surface topology (Fig. 2. 3) to some extent, and the head-field becomes flattened with the passage of time ST. I to III in turn. Meanwhile, judging from Fig. 4 .5, we can see the tendency that the estimation error is large in outer part of the region and appears small in center part, and of course, zero at the well points. The value of error becomes small rapidly with the passage of time. For instance, the value even in outer part reduces from several meters at ST. I to around 1 meter at ST. III. Fig. 4. 5 means that the spatial scale of available information which the observed point data give us, is gradually enlarged and the estimation accuracy of head-field are improved in the entire region because the randomness of the field after a rainfall reduces during dry period.

Since there are great uncertainty in the unconfined groundwater states just after rainfall, it is very difficult to estimate its spatial distribution of head-field with a limited number of observed data. As we have discussed, however, at the time stage in a long dry period, we can estimate the enough information on groundwater states in a region with rather greater scale even from rather small number of observations. In other words, the characteristics of randomness of groundwater behavior change to great extent with time, and then it turns out that the values of information given by the same observation system do change with the passage of time.

The kriging analysis based on the theoretical variogram will give us an useful tool to discuss the problems what kind of phenomena in time and space can be analyzed by the observed data in heterogeneous region or not.

Table 4. 1 Regression result of drift.

a_1	ST. I	ST. II	ST. III
a_1	19.41	24.30	26.10
a_2	0.051	0.025	0.016
a_3	0.076	0.042	0.026
a_4	9.8×10^{-6}	3.7×10^{-5}	4.9×10^{-5}
a_5	-1.2×10^{-4}	-6.9×10^{-5}	-3.2×10^{-5}
a_6	-1.3×10^{-4}	-7.3×10^{-5}	-7.5×10^{-5}
Var (m^2)	.520	.274	.094

drift : $m(X) = a_1 + a_2x + a_3y + a_4x^2 + a_5y^2 + a_6xy$

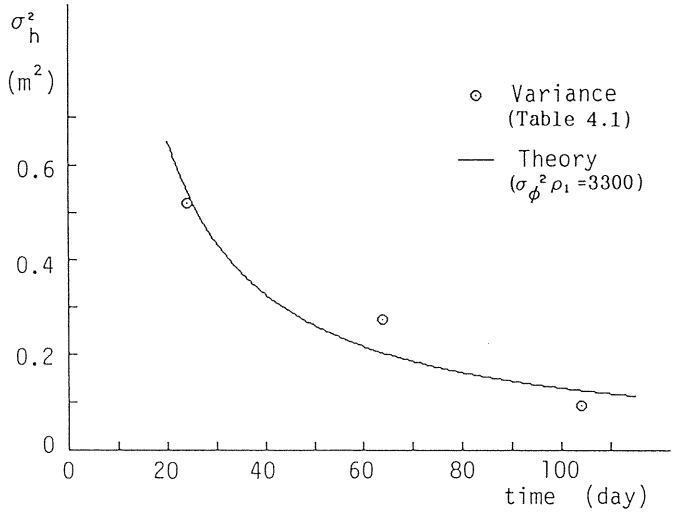

Fig. 4. 3 Comparison of residual variance with theoretical value of σ_h^2.

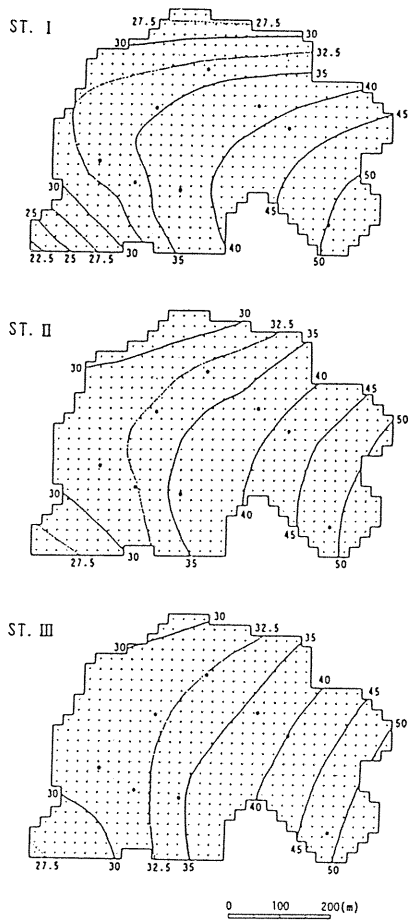

Fig. 4. 4 Kriging estimation of head-field (m).

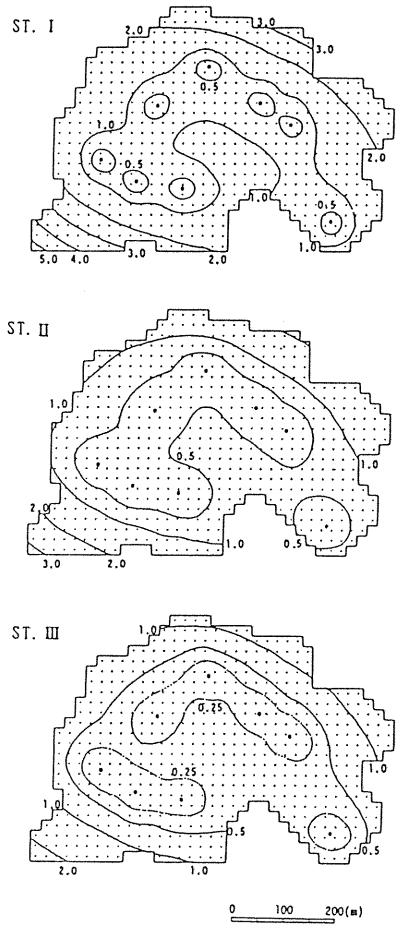

Fig. 4. 5 Kriging deviation for Fig. 4. 4 (m).

5. Inverse Analysis of Aquifer Parameter based on Uncertainty of Head

5. 1 Identification of Parameter in Heterogeneous Aquifer

Since the actual aquifer is a heterogeneous flow region in which the hydraulic permeabilities are distributed irregularly, the groundwater behavior is rather complex in space. While the head data in the groundwater observation are measured only at a limited set of the observation wells. The usual analysis of regional groundwater has been carried out on the basis of such the limited observation information, and then the aquifer parameters, such as the transmissivity T (or the permeability K) and the storativity S (or the specific yield Sy), have been identified by trial and error, so that the results of analysis fit to the observed head data. Recently, the inverse analysis methods, which estimate the optimum values of parameters for the observed data, have been developed for the more rational identification of parameters (Yeh, 1986). Even in these methods, the parameters are estimated on the basis of

the criterion that minimizes the difference between the observed head and the calculated head. Between these heads, however, the representative scales in space are so different each other, for the observed head is to considerable extent reflected by locality at the well point, while the calculated head is the numerical solution of the governing equation including macroscopic parameters under the simplified boundary conditions. Therefore, it is not necessarily possible to identify the exact values of parameters for the scale concerned by the conventional method that may compare the heads of different spatial scales. In this chapter, then, a new criterion is stated which enables us to utilize the uncertainty of head-field as the prior information in the identification process is proposed.

5. 2 *Objective Phenomena in This Inverse Analysis*

5. 2. 1 *Generation of Observed "Actual Phenomena"*

In order to discuss the problem what kind of identification method may give the more accurate estimation of the parameters, it is very difficult to choose the essential problems in the identification process from the actual groundwater behavior, since the actual phenomena are affected by various kinds of unknown factors. We will, therefore, discuss here the problems with respect to the "virtual but ideal phenomena" simulated in the computer through the linearized fundamental equation (Eq. (73)) for the horizontal two dimensional unconfined aquifer.

$$S(x,y)\frac{\partial h(x,y,t)}{\partial t} = \frac{\partial}{\partial x}\left[T(x,y)\frac{\partial h(x,y,t)}{\partial x}\right] + \frac{\partial}{\partial y}\left[T(x,y)\frac{\partial h(x,y,t)}{\partial y}\right] + Re \tag{73}$$

where $h(x,y,t)$ is the unconfined head, $T(x,y)$ is the transmissivity, $S(x,y)$ is the specific yield and Re is the recharge intensity due to rainfall.

For the case study, let us consider at first on the conditions that generate the virtual observed data, on which the identification process is discussed. From the view point of frequency distribution of the aquifer parameters, transmissivity T and specific yield S, the flow region may be essentially classified into four cases as shown in Fig. 5. 1. As the first case, the region is the ideally homogeneous one with the identical values of the aquifer parameters as the distribution (I). Second case: the parameters T and S follow the lognormal and the normal distributions, respectively, as stated in chapter 2. This case may be conceptually expressed as the distribution (II). If the region concerned consists of some geological subregions, the frequencies of T and S become as Figs. (III) or (IV). Figs. (III) and (IV) correspond to the cases in which the sub-regions are ideally homogeneous and heterogeneous, respectively. In the case study here we will consider the aquifers which have its frequency distributions of parameters stated in the cases of (I) and (II). The values of transmissivity $T(x,y)$ and specific yield $S(x,y)$ are generated from the following populations for each finite element of analysis domain.

homogeneous region (I) : $T(x,y) = 100\ (\mathrm{m}^2/\mathrm{day})$, $S(x,y) = 0.2$

heterogeneous region (II) :

$T(x,y)$: lognormal pdf with $E[\log_{10}T] = 2.0$ and $\mathrm{Var}[\log_{10}T] = 0.05$
$S(x,y)$: normal pdf with $E[S(x,y)] = 0.2$ and $\mathrm{Var}[S(x,y)] = 0.005$

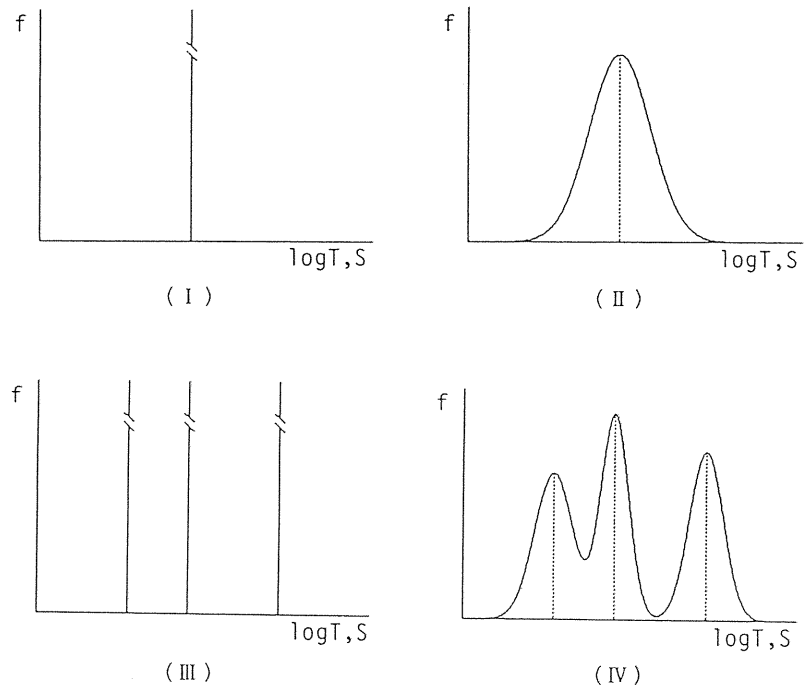

Fig. 5. 1 Frequency distribution of aquifer parameters.

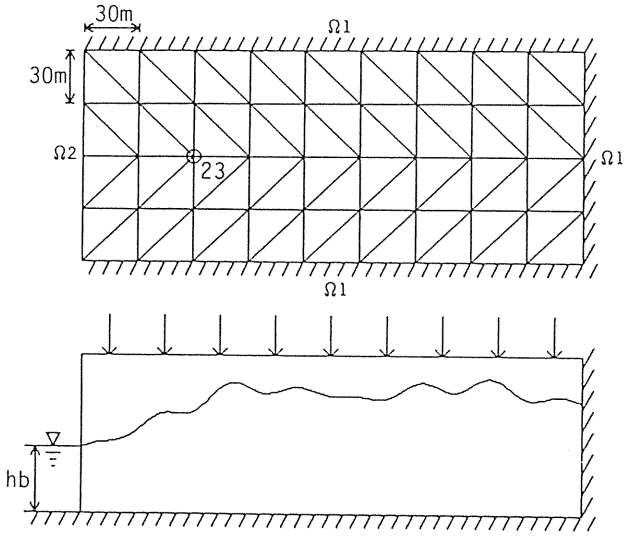

Fig. 5. 2 Virtual unconfined aquifer for simulation of phenomena.

It is also supposed in the case study that the rainfall pours with a strong intensity in a short period, and that a long dry period follows after the rainfall. And the recharge intensity Re due to rainfall is given as

$Re = 83$ mm/hr for $t < 0.5$ day
$Re = 0$ for $t > 0.5$ day

While the initial and boundary conditions are given as follows

Initial condition : $h(x,y,0) = h_0$ (=10 m)
Boundary condition : $\partial h/\partial n = 0$ ($\Omega \in \Omega_1$), $h(x,y,t) = h_b$(=10 m)($\Omega \in \Omega_2$)

in which Ω_1 and Ω_2 are the boundaries of the region shown in Fig. 5. 2. For these conditions, the virtual observed head data are generated by sampling from the numerical results of FEM analysis based on the fundamental equation (1) for the aquifer, as shown in Fig. 5. 2.

5. 2. 2 *Identified Equivalent Aquifer Model*

As mentioned above, the aquifers considered in this analysis are a homogeneous aquifer (I) with the constant parameters and a heterogeneous aquifer (II) with the parameters fluctuating a little in the neighborhood of their averages. The simulated head values at several fixed points in the region are considered as the "virtual" observed heads. And then, based on these observed head data, the equivalent homogeneous model is identified in engineering sense to estimate constant model-parameters for the region as a whole. The fundamental equation of the equivalent homogeneous model is then as follows.

$$So\frac{\partial h^*(x,y,t)}{\partial t} = To\left[\frac{\partial^2 h^*(x,y,t)}{\partial x^2} + \frac{\partial^2 h^*(x,y,t)}{\partial y^2}\right] + Re \tag{74}$$

where $h^*(x,y,t)$ is the head in the equivalent aquifer, To and So are the equivalent parameters (spatially constant) identified, and Re is the recharge intensity. If the inverse analysis is carried out during the dry period (no rainfall), it is impossible to identify To and So independently because of $Re = 0$, and becomes possible to identify only the ratio To/So. Therefore, the inverse problem in this research treats the identification of the parameter To/So in the equivalent aquifer, based on the unsteady head data observed in the "actual aquifers" (I) and (II).

5.2.3 *Observation System and "Virtual" Observed Data*

The groundwater investigations in the actual field are limited in quality and quantity by some restriction. Fig. 5. 3 indicates a general existence situation of the observed head data. As found in this figure, the head investigations carried out actually are the continuous time observations at a few points ($X_i, X_j, \cdots$), or the simultaneous observation at a large number of points at a few times ($t_l, t_m, \cdots$) using existing wells. That is, it is impossible to observe the head behaviors at all time and in whole space in usual investigations. Taking these conditions into consider, the following two kinds of the head data (a) and (b), observed in the aquifers (I) and (II) respectively, are treated as the base of this inverse analysis.

(a) Continuous time data at a node
(b) Simultaneous data at all nodes at two time stages

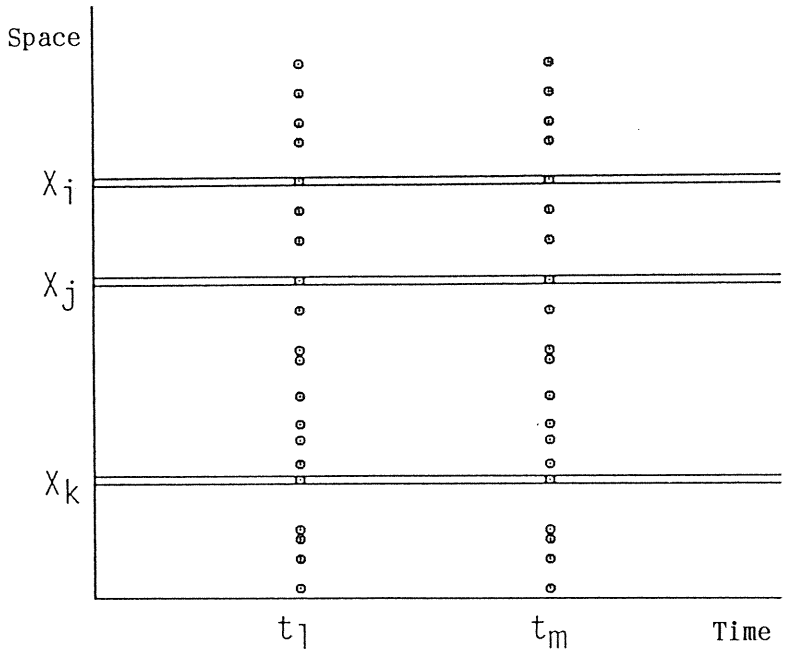

Fig. 5. 3 General existence situation of observed head data.

5. 3 *Conventional Criterion for Parameter Identification and Its Problems*

5. 3. 1 *Formulation of Inverse Problem*

The conventional criterion for the parameter identification may be stated as to minimize the following objective function,

$$J_1(P_1, P_2, \cdots, P_l) = \sum_{i=1}^{m} (h_i^{obs} - h_i^{cal})^2 \rightarrow \min. \tag{75}$$

In this equation, h^{obs} describes the observed head, h^{cal} : the calculated head, m : the number of observed values, P : the model parameter and l : the number of parameters. In case of Eq. (74), $l = 2$, then $P_1 = To$ and $P_2 = So$. To overcome the difficulty of the nonlinearity of the optimization problem Eq. (75), Gauss-Newton method is adopted. That is, after linearizing the function $h(P)$ in the neighborhood of parameter P, the following normal equation is derived by the condition of $[\partial J_1 / \partial P_j] = 0$.

$$\sum_{k=1}^{l} \sum_{i=1}^{m} Q_{ij} Q_{ik} \cdot \triangle P_k = \sum_{i=1}^{m} (h_i^{obs} - h_i^{cal}) \cdot Q_{ij}, \quad j = 1, 2, \cdots, l \tag{76}$$

in which Q is the Jacobian matrix of head for parameters,

$$Q_{ij} = \frac{\partial h_i^{cal}}{\partial P_j} \tag{77}$$

and $\triangle P$ is correction value of P. Jacobian Q is estimated by the following forward difference approximation.

$$Q_{ij} = \{h_i^{cal}(P_j + \delta P_j) - h_i^{cal}(P_j)\} / \delta P_j \tag{78}$$

where $\delta P_j = \delta_j \cdot P_j$, δ_j is constant.

This inverse analysis is carried out by the following procedures. At first, after giving the initial values (first approximation) of P_j and δ_j, Jacobian matrix is calculated by the numerical analysis of fundamental equation (74) for the equivalent model. Then, the correction values of parameters are estimated by the normal equation (76). The initial values then are improved and the process is iterated to get the correction values which satisfy the following condition.

$$\triangle P_j < \varepsilon_j \tag{79}$$

where ε_j is a constant index of convergence, $\varepsilon_j = P_j / 200$. The values of δ_j are here assumed to be $\delta_1 = 0.0001$ and $\delta_2 = 0.1$.

5. 3. 2 *Inverse Analysis based on Criterion J_1*

Based on the conventional criterion, the results of identification of the parameter To/So in equivalent model for the aquifers (I) and (II) are discussed. In the case of the homogeneous aquifer (I), the identification of To/So corresponds to evaluate true value of T/S in actual aquifer. Therefore, if the parameter is identified correctly, the calculated head $h^{cal}(= h^*)$ should be equal perfectly to the observed head h^{obs}. Fig. 5. 4 shows the identification processes : (a) is the results on the basis of the daily "data" for 5 days at node No. 23 in Fig. 5. 2, and (b) is the results for the "data" at all nodes at 5 and 10 days after rainfall. True value of T/S is given as $500(= 100/0.2)\text{m}^2/\text{day}$. From these figures, it has been clarified that estimated value perfectly converges to 500 m^2/day by iteration within 3 to 5 steps and that the inverse analysis for the homogeneous region is successfully carried out, whenever the initial value of To/So is taken as 1000, 750 and 250 (m^2/day).

In the mean time, since the aquifer (II) is of the case that T/S has the random distribution with a constant average value, To/So in the equivalent model corresponds to the expected value of T/S, $E[T/S]$. The results of the inverse analyses based on the same observed data as Fig. 5. 4 are shown in Fig. 5. 5. Although the true value of $E[T/S]$ is given as 500 (m^2/day), the identified values do not converge to it for both the data (a) and (b), and then the solutions become to diverge in the iterations. It seems that these results are caused by the uncertain components included in the observed head due to the heterogeneity of aquifer (II). As we have already discussed, the randomness of head-field reduces gradually during the dry period, but in the more heterogeneous aquifer it remains and does not vanish perfectly. The identification here has been made under this situation. The divergency of results in Fig. 5. 5, especially (b), are caused from the identification process where all head data are handled with same weight on the criterion J_1, disregarding the fact that the randomness of head changes between two time stages of the observation. That is, if the region is heterogeneous, it may be stated that the conventional criterion can give not always the accurate estimation of parameters. In next section, then, a new criterion in terms of the statistical properties of the uncertainty of head due to the heterogeneity in flow region is proposed.

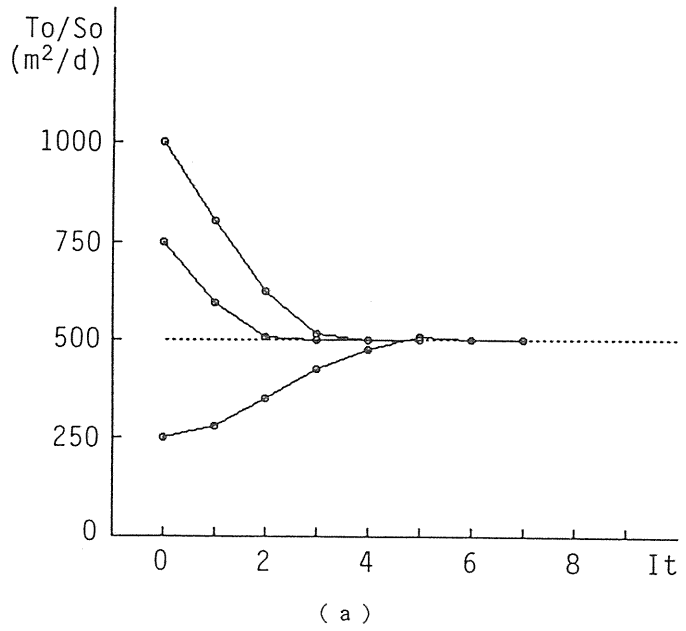

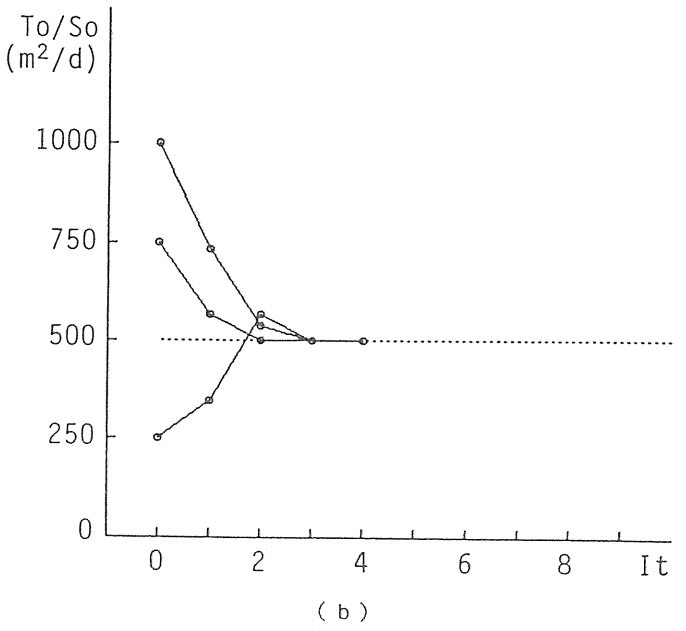

Fig. 5. 4 Identification process based on criterion J_1 for aquifer (I).
(a) by daily data for 5 days at a node (No. 23 in Fig. 5. 2)
(b) by data at two time stages (5 and 10 days after rainfall) at all nodes

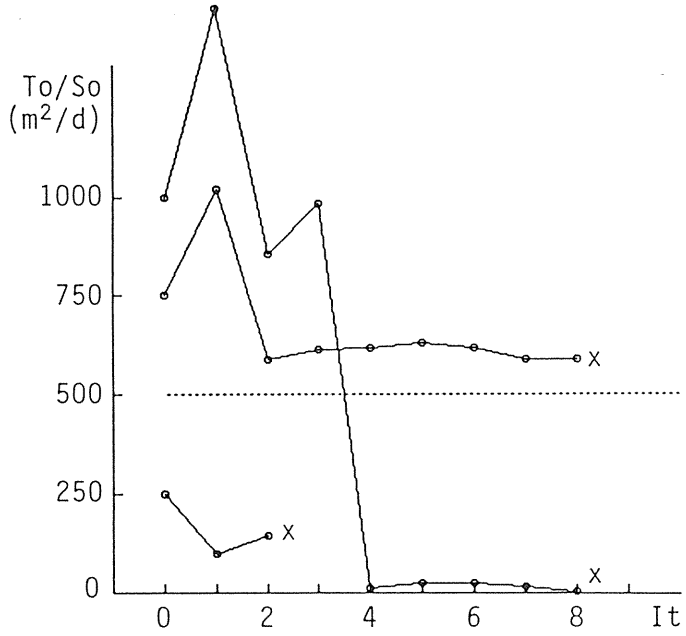

(a)

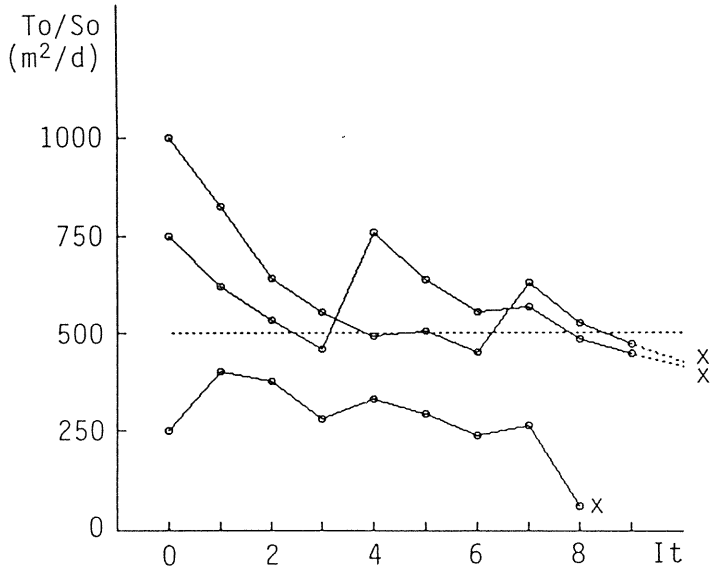

(b)

Fig. 5. 5 Identification process based on criterion J_1 for aquifer (II).
(a) by daily data for 5 days at a node (No. 23 in Fig. 5. 2)
(b) by data at two time stages (5 and 10 days after rainfall) at all nodes

5. 4 *A New Method for Inverse Analysis of Heterogeneous Aquifer*

5. 4. 1 *Criterion of Identification based on Head Variance*

In chapter 4, the stochastic spatial structure of head-field for the two dimensional unconfined aquifer has been evaluated by combining the physical laws and the statistical concept. Its objective phenomenon was such the smoothing process of head that the random head-field after a strong storm calms down during a long dry period. In other words, the phenomena treated in the previous chapter may be understood as same as the phenomena in the aquifer (II), which should be here identified. That is, the knowledge obtained in chapter 4 may be successfully applied to the identification of the aquifer (II), though the knowledge has been derived from some assumptions. From the theoretical form of the head variogram (Eq. (65)) in smoothing process, the time evolution of the head variance can be expressed in the following equation.

$$\sigma_h^2(t) = \frac{\sigma_\phi^2 \rho_1}{8\pi\lambda_0 t} \tag{80}$$

where $\sigma_h^2(t)$: the head variance at time t, σ_ϕ^2 : the head variance just after rainfall, λ_0 : the average diffusivity ($= E[T(x,y)/S(x,y)]$) and ρ_1 : a constant.

While, the original definition of the head variance is

$$\sigma_h^2(t) = E[\{h(x,y,t) - E[h(x,y,t)]\}^2] \tag{81}$$

Since $E[h(x,y,t)]$ is the head in homogeneous region, it corresponds to the calculated head in the equivalent model here concerned, namely $h^{cal}(= h^*)$. Therefore, Eq. (81) means the temporal behavior of the mean square of difference between the observed head and the head calculated with the parameters identified correctly. That is, for the correct parameters $E[(h^{obs} - h^{cal})^2]$ should be equal to σ_h^2 in Eq. (81). Therefore, for these correct parameters $E[(h^{obs} - h^{cal})^2]$ is also equal to σ_h^2 in Eq. (80). This relationship may be then rewritten into the following new criterions for the parameter identification (Harada & Takagi, 1989).

$$J_2(P_1,P_2) = \sum_{i=1}^{N} \{\sigma_h^2(t_i) - \sigma_{h^*}^2(t_i)\}^2 \rightarrow \min. \tag{82}$$

where $\sigma_h^2(t)$ is theoretical head variance (Eq. (80)), $\sigma_{h^*}^2(t)$ is the calculated head variance, and N is the number of time stages at which the head variance are calculated. If the simultaneous observations are made at M points, $\sigma_{h^*}^2(t)$ can be estimated from the following equation.

$$\sigma_{h^*}^2(t_j) = \sum_{i=1}^{M} \{h_i^{obs}(t_j) - h_i^{cal}(t_j)\}^2 / M \tag{83}$$

The above objective function J_2 proposed here is a new criterion based on the temporal behavior of the statistical quantity as the head variance, while the function J_1 has been on the basis of conformity of the head itself. In this criterion, the theoretical behavior of head variance are utilized as the prior information for the inverse analysis.

5. 4. 2 Inverse Analysis of Aquifer (II) based on Criterion J_2

Let us apply the above criterion J_2 to the heterogeneous aquifer (II), for which the parameter could not be identified by the criterion J_1. Using Gauss-Newton method as the procedure of optimization, the normal equation becomes as follows.

$$\sum_{k=1}^{2}\sum_{i=1}^{N} U_{ij}U_{ik}\cdot\triangle P_k = \sum_{i=1}^{N}\{\sigma_h^{\,2}(t_i) - \sigma_{h^*}^{\,2}(t_i)\}\cdot U_{ij}, \quad j=1,2 \tag{84}$$

where U is the Jacobian matrix of head variance for the parameters,

$$U_{ij} = \frac{\partial \sigma_{h^*}^{\,2}(t_i)}{\partial P_j} \tag{85}$$

It is necessary for the calculation of Eq. (84) to determine the unknown coefficient $\sigma_\phi^{\,2}\rho_1$ involved in $\sigma_h^{\,2}(t)$. If the parameter *To/So* in the equivalent model is estimated correctly, the calculated value of the head variance at $t = t'$ should be equal to the theoretical one, that is, $\sigma_h^{\,2}(t') = \sigma_{h^*}^{\,2}(t')$. Therefore, the unkown coefficient in Eq. (80) is obtained as Eq. (86) and then theoretical variance $\sigma_h^{\,2}(t)$ may be replaced by Eq. (87).

$$\sigma_\phi^{\,2}\rho_1 = 8\pi\cdot E[T/S]\cdot\sigma_{h^*}^{\,2}(t')\cdot t' \tag{86}$$

$$\sigma_h^{\,2}(t) = \sigma_{h^*}^{\,2}(t')\cdot t'/t \tag{87}$$

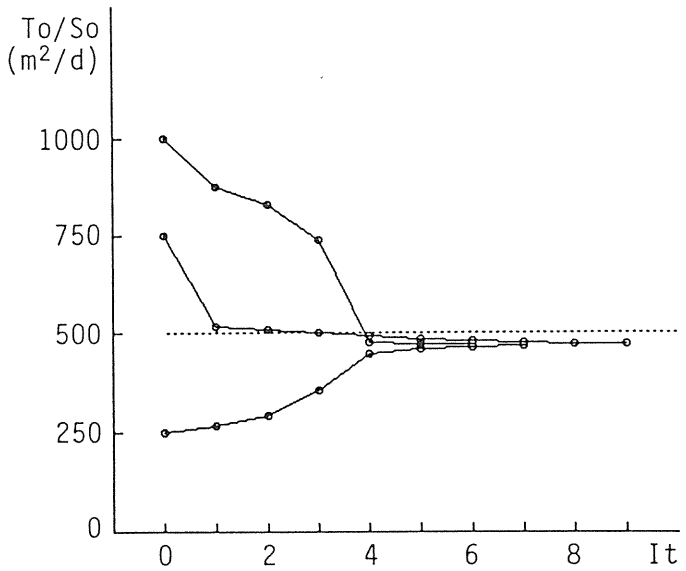

Fig. 5. 6 Identification process based on criterion J_2 for aquifer (II) by data at two time stages (5 and 10 days after rainfall) at all nodes.

For the case that the observation of head is carried out at all nodes at two time stages $t = 1$ and 5 (day) after rainfall, $N = 2$ in Eq. (82) and $M = 50$ in Eq. (83). Fig. 5. 6 shows the result of inverse analysis. In the case the unknown coefficient has been determined at the first observation time: $t' = 1$(day). According to this figure, we can see the fact that the identified value of To/So converges to a constant value in the iterations of 5 to 7 steps. The final convergence value is about 470 (m^2/day), a little smaller than true value of $E[T/S]$: 500 (m^2 /day). In this way, we can estimate the accurate parameters in the case, for which the criterion J_1 has resulted in a failure. The error of the estimated value may be understood as to depend mainly on the difference of conditions between the aquifer (II) and the infinite aquifer on which the theoretical variance has been analyzed. Although these problems remains to be solved, what we would like to emphasize here is the fact that the equivalent parameter for heterogeneous aquifer can be identified with good accuracy by the criterion J_2 based on the head variance.

6. Concluding Remarks

This study is aimed at stochastic evaluation of the uncertainty of unconfined groundwater behavior in the heterogeneous region due to a heavy rainfall. The results obtained through the study are summarized as follows:

(a) The head variance which statistically expresses the spatial randomness of water table response to a rainfall has been formulated with the help of both flow properties in the unsaturated zone and in the aquifer.
(b) Through the evaluation of head variance, the fact that the head-field has greater randomness of spatial distribution in the silty aquifer than in the sandy aquifer is demonstrated.
(c) The unsteady head variogram after a rainfall has been formulated by evaluating the random component of head due to the heterogeneity of flow region based on the physical laws of groundwater.
(d) As the result of kriging estimation in the practical region, it is clarified that although the estimation error of head-field is very large just after rainfall, the error decreases during a dry period, that is, the estimation accuracy of the field is gradually improved.
(e) A new criterion for the parameter identification in the regional groundwater modelling, which takes full advantage of the statistic property on the uncertainty of actual head behavior, is proposed.

The discussions in the present paper are closely connected with some essential problems in groundwater hydrology, such as mathematical analyses combining the physical and statistical characteristics of phenomena involving the treatment of the heterogeneity, evaluation of observed data relating with the spatial and temporal scales of phenomena, the identification of the equivalent model and so forth. The extention of the research works in this direction may develop a new methodology to analyze the characteristics of groundwater behavior in actual heterogeneous region, utilizing the information on geological and geophysical properties.

References

1) Akaike, H. (1973) Information theory and an extention of the maximum likelihood principle, *Proc. 2nd Inter. Symp. on Information Theory* (Petrov, B.N. & Csaki, F. eds.), Akademiai Kiado, Budapest, 267-281.
2) Brooks, R.H. & Corey, A.T. (1966) Properties of porous media affecting fluid flow, *Proc. ASCE, 92 (IR2)*, 61-88.
3) Dagan, G. (1982) Analysis of flow through heterogeneous random aquifers, 2. Unsteady flow in confined formations, *Wat. Resour. Res., 18 (5)*, 1571-1585.
4) Dagan, G. & Bresler, E. (1983) Unsaturated flow in spatially variable fields, 1. Derivation of model of infiltration and redistribution, *Wat. Resour. Res., 19* (2), 413-420.
5) Delhomme, J.P. (1978) Kriging in the hydrosciences, *Advances in Water Resources, 1 (5)*, 251-266.
6) Delhomme, J.P. (1979) Spatial variability and uncertainty in groundwater flow parameters: A geostatistical approach, *Wat. Resour. Res., 15* (2), 269-280.
7) Freeze, R.A. (1975) A stochastic-conceptual analysis of one-dimensional groundwater flow in non-uniform homogeneous media, *Wat. Resour. Res., 11* (5), 725-741.
8) Harada, M. & Takagi, F. (1989) A stochastic approach to the inverse problem of unconfined heterogeneous aquifer, *Proc. 33th Japanese Conf. on Hydraulics*, 217-222 (in Japanese).
9) Journel, A.G. & Huijbregts, CH.J. (1978) "Mining Geostatistics", Academic Press, London.
10) Richards, L.A. (1931) Capillary conduction of liquids through porous mediums, *Physics, 1*, 318-333.
11) Takagi, F., Harada, M. & Uchida, K. (1985) On the characteristics of groundwater behavior in the Komaki hill region, *J. of Japanese Association of Groundwater Hydrology, 27 (4)*, 171 -182 (in Japanese).
12) Takagi, F. & Harada, M. (1988) Stochastic estimation of groundwater head-field in heterogeneous region, *Proc. 6th Congr. APD-IAHR*, Kyoto, vol.II, 477-484.
13) Yeh, W.W-G (1986) Review of parameter identification procedures in groundwater hydrology : the inverse problem, *Wat. Resour. Res., 22 (2)*, 95-108.

Nomenclature

a_l	: Coefficient of the polynomial drift function
$C(x,y)$	: Heterogeneity coefficient of unsaturated zone
$Cov[\cdot]$	: Covariance function in random field
d	: Spatial distance between two any points
D	: Area of the domain concerned
D or Dp	: Depth from ground-surface to groundwater-table
D'	: Depth to upper-limit of capillary zone
$E[\cdot]$	: Expect value of random variable
$f^l(\mathbf{X})$	: Polynomial function for drift $m(\mathbf{X})$
$G(x,y,t)$	: Green function of the diffusion equation
$h_0(x,y,t)$	: $H'(x,y,t)$ in homogeneous region
$h_1(x,y,t)$	: Random head component due to heterogeneity of region
$H(x,y,t)$	: Water depth on impermeable base
$H'(x,y,t)$	: Difference between $H(x,y,t)$ and H_0 ($= h_0 + h_1$)
H_0	: Temporal and spatial average value of $H(x,y,t)$
J_1 or J_2	: Criterion for inverse problem of aquifer parameters
k	: Number of terms in drift function
K	: Unsaturated or saturated permeability
Ks	: Saturated permeability

L : Length to wetting front in equivalent moisture profile
L_f : Length to wetting front in actual moisture profile
$m(\mathbf{X})$: Drift or trend of random variable
P : Model parameter
Pe : Effective porosity of unsaturated soil
q : Moisture flux in unsaturated zone
q_0 : Moisture flux into soil at ground-surface
q^* : Moisture flux in equivalent profile
Q : Jacobian matrix of head
R : Total volume of rainfall, or recharge intensity
$R(\mathbf{X})$: Residual component except drift in random field
Ra : Rainfall intensity on ground-surface
Re : Recharge intensity on groundwater-table
S : Storativity or effective porosity of aquifer
Se : Effective saturation
So : S in the equivalent aquifer
Sy : Specific yield
t : Time
tr : Rainfall duration
T : Transmissivity ($= KsH_0$)
To : T in the equivalent aquifer
U : Jacobian matrix of head variance
$V(t)$: Increased volume of soil moisture
$Var[\cdot]$: Variance of random variable
W : Weighting coefficient of kriging
x : Location axis
$\mathbf{X}$: Location vector
y : Location axis
Y : Logarithm of transmissivity ($= \log T$)
z : Location axis
$Z(\mathbf{X})$: Random variable at location $\mathbf{X}$
$\hat{Z}(\mathbf{X})$: Best Linear Unbiased Estimator (BLUE) of Z
β : Parameter of unsaturated moisture property
γ : Semi-variogram
$\delta(\cdot)$: Dirac's delta function
ε : Index of convergence in iteration process
η : Parameter of unsaturated moisture property
θ : Volumetric moisture content
θ_n : Field capacity
θ_r : Minimum moisture content
θ_s : Saturated moisture content
λ_o : Average diffusivity
ρ_h : Auto-correlation function of h
ρ_ϕ : Auto-correlation function of ϕ
ρ_Q or ρ_1 : Constant on the white noise assumption
σ_{cs}^2 : Summation of variances of $C(x,y)$ and $S(x,y)$
σ_h^2 : Head variance
ϕ : Random head distribution just after rainfall
Φ : Total head of unsaturated flow
ψ : Capillary head
ψ_w : Air entry value
$\triangle H$: Rising height of water-table